Prediction of Sloshing Noise in Rectangular Tank

Agawane Girish Babanrao

Under the guidance of

Dr. B.Venkatesham
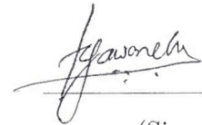
भारतीय प्रौद्योगिकी संस्थान हैदराबाद
Indian Institute of Technology Hyderabad

Department of Mechanical Engineering

June 2014

Declaration

I declare that this written submission represents my ideas in my own words, and where ideas or words of others have been included, I have adequately cited and referenced the original sources. I also declare that I have adhered to all principles of academic honesty and integrity and have not misrepresented or fabricated or falsified any idea/data/fact/source in my submission. I understand that any violation of the above will be a cause for disciplinary action by the Institute and can also evoke penal action from the sources that have thus not been properly cited, or from whom proper permission has not been taken when needed.
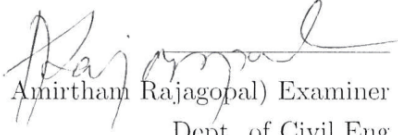
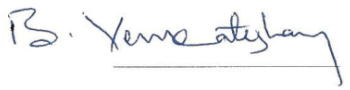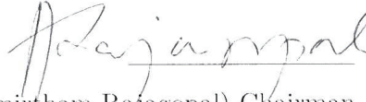(Signature)

(Agawanc Girish Babanrao)

ME12m1001

(Roll No.)

Approval Sheet

This Thesis entitled Prediction of Sloshing Noise in Rectangular Tank by Agawane Girish Babanrao is approved for the degree of Master of Technology from IIT Hyderabad

(Dr. Amirtham Rajagopal) Examiner
Dept. of Civil Eng
IITH

(Dr. Raja Banerjee) Examiner
Dept. of Mechanical Eng
IITH

(Dr.B.Venkatesham) Adviser
Dept. of Mechanical Eng
IITH

(Dr. Amirtham Rajagopal) Chairman
Dept. of Civil Eng
IITH

Acknowledgements

Abstract

With significant decrease in the background noise in present day automobiles, liquid slosh noise from an automotive fuel tank is considered as a great irritant during acceleration and deceleration. All major international OEMs and their suppliers try to reduce sloshing noise by various design modifications in the fuel tank. However, most major activities reported in open literature are primarily based on performing various CAE and experimental studies in isolation. At the same time, noise generation and its propagation is a multiphysics phenomenon, where fluid mechanics due to liquid sloshing affects structural behaviour of the fuel tank and its mountings which in turn affects noise generation and propagation. In the present study, a multiphysics approach to noise generation has been used to predict liquid sloshing noise from a rectangular tank. By taking Computational Fluid dynamics (CFD)data, Finite Element Analysis (FEA) and Boundary Element Method (BEM) simulation studies have been performed in a semi-coupled manner to predict noise. Sloshing noise generated due to fluid interaction with structural walls is simulated using Vibro-acoustic model. An integrated model is developed to predict dynamic forces and vibration displacement on tank walls due to dynamic pressure loading on tank walls. Noise radiated from tank walls is modelled by Harmonic Boundary Element Method and transient Finite Element method. Experimental and numerical studies have been performed to understand the mechanics of sloshing noise generation. Images from high speed video camera and noise measurement data have been used to compare numerical result.

Contents

Chapter 1

Introduction

1.1 Definition

Liquid fuel in a partially filled automotive tank oscillates when subjected to sudden acceleration or deceleration. This low frequency oscillation of free surface is called liquid sloshing and is one of the source of noise generation in an automobile. Due to sloshing, complex surface waves are generated and dynamic forces are exerted on the tank walls. This results in noise generation which is typically referred as sloshing noise.

Figure. 1.1 shows the classification of sloshing noise and its generation mechanism
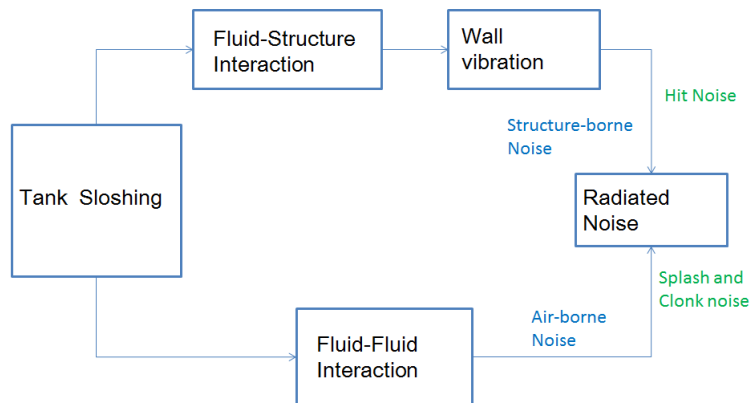
Figure 1.1: Sloshing noise classification

1. Noise radiation due to tank wall vibration

   Figure.1.2a shows the hitting phenomenon inside the tank. This noise occurs when fuel moves to one side of the tank and strongly strikes the inner wall due to the force exerted on it by vehicle braking this is also known as fluid-structure interaction. The vibration that occurs in the tank is mainly transferred as structure-borne vibration

that is heard as sloshing noise at the observation location. The noise due to fluid-structure interaction is also known as hitting noise and it occurs generally at lower frequencies 50 Hz to 500 Hz frequency range.
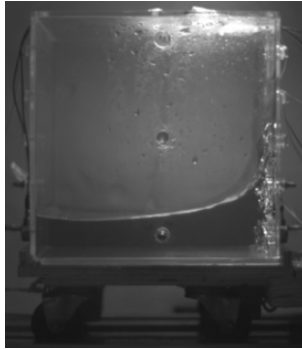
(a) Hitting
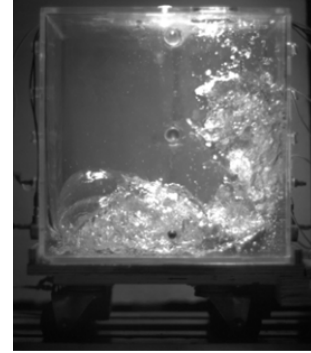
(b) Splashing

Figure 1.2: Sloshing events

2. Noise resulting from fluid-fluid interaction

Figure.1.2b shows the splashing phenomenon inside the tank, this noise is also known as air-borne noise.When a vehicle stops due to sudden braking, this noise occurs as a result of the (fluid-fluid interaction) fuel impacting itself , or interacting with air, which creates pressure pulses inside the fuel tank. It is mainly transmitted as air-borne noise that transmits exterior through tank walls. The noise due to fluid-fluid interaction is known as splashing noise, generally it occurs at higher frequencies 500 Hz to 10 kHz.

3. Clonk noise

This type of noise is generated when abrupt compression of air by sloshing liquid takes place. It's intensity as well as application time is lowest among the three and it occurs in the frequency range of 150-500 Hz.

1.2   Motivation

Due to dramatic minimization of other sources of noise generation in an automobile like exhaust, power train, tyre and air-borne noise, noise generation due to sloshing in the fuel tank is getting increased attention as it is considered to be an irritant for the passenger in the vehicle.

The sloshing noise which passengers can hear is produced in a quiet driving condition such as parking their cars in an quiter parking lot. Sloshing is complicated problem and generally treated numerically as fluid structure interaction problem. Sloshing has plenty of application in automotive, marine transportation, aerospace.

2

Many factors influence slosh noise performance, including:

1. Fuel Tank material properties like elasticity, density and stiffness,

2. Fuel type and fill level,

3. Vehicle acceleration and deceleration level,

4. Interior geometry of the tank shell (eg.baffes,pads etc.),

5. Other objects inside the tank which are impacted by moving fuel.

Therefore, a simulation to predict slosh noise should include these critical parameters.

1.3   Literature Survey

Based on their experimental work, Wachowski et al [1] classified sloshing noise into three categories: Splash, Hit and Clonk noise. Each of these three categories of noise occur at distinct range of frequencies and is found out using wavelet analysis. They concluded optimisation of the tank structure can achieve lower noise emission and vibration.

Kamei et al [2] determined a sloshing noise correlation that relates factors pertaining to the fuel tank, body parts and tank mounting structure. The tank mounting structure which is related to both the fuel tank and the body parts has the largest contribution to sloshing noise. Also he catagorized the low frequency structure borne noise and high frequency air borne noise.

Kamiya et al [3] used coupled analysis to study interaction between fluid and structure models to predict sloshing using MSC.Dytran. They studied effect of baffle configurations and fluid level on sloshing dynamics.

De Man and Van Schaftingen [4] performed a source-path-receiver analysis for both structural and air borne noise for a sloshing fuel tank.

Wiesche [5] derived a correlation between slosh noise pressure fluctuations within the sloshing liquid. He used two-phase Computational Fluid Dynamics (CFD) to track liquid interface within realistic tank geometries to determine these pressure fluctuations. He discussed effect of anti-slosh element (Baffles and pads) on the slosh dynamics. However prediction about the absolute sound level cannnot be made.

Park et al [6] used a Fluid Structure Interaction (FSI) approach to predict noise due to sloshing. Also they carried out numerical optimization of parameters to reduce computation time.

Vytla and Ando et al [7] performed a one-way coupled FSI analysis. They studied the effect of deceleration magnitude for different fuel tank fill level.

Khezzar et al. [8] studied sloshing in rectangular tank subjected to impulsive force and concluded that flow visualization of experimental and numerical simulation were similar.

Hattori et al [9] studied different types of waves generated due to sloshing and classified them on the basis of impact pressure pattern achieved during experimentation with a specific type of wave.

Thiagrajan et al. [10] worked on sloshing in a rectangular tank using sway excitation and observed that 20 % and 80 % of fill level, causes higher pressure than other condition.

Hou et al. [11] applied multiple excitations on a rectangular tank and concluded that liquid sloshing become violent and intensified if sloshing tank is under multiple coupled excitations.

Peric and Zorn [12] studied structural impact of sloshing loads caused by arbitrary motion of tank. The numerical simulation shows agreement with the experiment. It is also found that there is negligible difference between result in turbulence and laminar model.

Jaiswal et al [13] have conducted Experimental and numerical studies on sloshing and have obtained the sloshing frequency of liquid contained in tanks of other shapes and tanks with internal obstructions using Electro-Magnetic Shake Table and ANSYS software.

It is still well accepted that the mechanism of noise generation due to sloshing is not well understood. However, slosh noise prediction and its prevention is important from fuel tank design point of view.

1.4   Outline of thesis

1. *Chapter 1* , main motivation behind this work is explained. This includes need to study the effect of sloshing noise in automobile. Types of sloshing, mechanism of sloshing noise generation is explained in first chapter. Extensive literature survey is presented to support reserch work.

2. *Chapter 2* , includes theoretical background of different analysis and principles used for reserch work. Analysis part contains modal analysis, transient dynamic analysis, acoustic analysis. Selection criteria of field points, different coupling methods used in sloshing simulation are explained brief in *chapter2*

3. *Chapter 3*, briefly explains experimental setup used for sloshing studies. Impact test setup is designed to simulate actual test condition in automobile. Different subsystems and their details are expalined in this chapter. Subsystem contains braking system, loading system, track-vehicle and instrumentation.

4. *Chapter 4* is related with numerical analysis techniques. As sloshing noise prediction is multi-physics problem and which includes CFD analysis, Structural analysis and acoustic analysis. In chapter 4, simulation methodology for this FSI problem and different approach to solve are explained. Acoustic transient and harmonic analysis methods are briefly explains in this chapter.

5. *Chapter 5* explains experimental and numerical results. Different parametric studies have been carried out to understand sloshing inside the tank. Effect of fill level, deceleration and sensor locations on sloshing parameters is briefly explained. FSI simulation and acoustic simulation results are presented in this chapter.

6. *Chapter 6*, concludes the reaserch work and directions to proceed sloshing study further.

Chapter 2

Theoretical Background

Sloshing noise analysis is a multiphyics problem. So, it is essential to understand different approaches to solve this problem, basic governing equations and principles for different analysis technique like modal analysis, transient dynamic analysis and acoustic analysis.

2.1 Modal analysis

Modal analysis is used to determine the dynamic/vibration characteristic of system. Modal analysis determines the natural frequency, mode shapes and mode participation factor (how much a given mode participates in a given direction). Natural frequency and mode shapes are important parameters in the design of structure for dynamic loading condition like transient loading, harmonic loading etc. Assumptions considered for modal analysis are, structure has constant stiffness and mass effect, no damping, no time varying forces and pressure acting on structure (pressure). For sloshing problem, modal analysis is performed in order to demonstrate the contribution of the structural properties of the tank in the slosh noise prediction. The equation of motion for undamped system expressed in matrix notation [14]

$$[M]\{\ddot{u}\} + [K]\{u\} = \{0\} \tag{2.1}$$

For linear system, free vibration will be harmonic of the form

$$\{u\} = [\phi]_i \sin \omega_i t$$

where,

$[\phi]_i$ = eigenvector representing mode shape of the ith natural frequency

ω_i = i^{th} circular natural frequency (radians per unit time)

t = time

Thus the equation of motion becomes,

$$(-\omega_i^2[M] + [K])\{\phi_i\} = \{0\}$$

The above condition is satisfied only when determinant of $(-\omega_i^2[M]+[K])$ is zero because the other condition $\{\phi_i\} = \{0\}$ gives trivial solution.

Thus,

$$[-\omega_i^2[M] + [K]] = 0$$

This is eigen value problem may be solved upto n values of natural frequencies and n values of mode shapes where n is number of degrees of freedom.

2.2   Transient dynamic analysis

Transient dynamic analysis is a technique used to determine the dynamic response of structure under the action of any time-dependent loads. Output of this analysis is used to determine time-varying displacement, strain, stress etc. The project work involves the transient dynamic analysis which determines transient response of structure under the action of impulsive load due to liquid sloshing on the walls of the tank. The load which acts on structure for small duration of time with high value of magnitude is charactrised as impulsive load. Since an ideal impulse force excites all modes of a structure.

The basic governing equation of motion for multi-degree freedom system is given as [14],

$$[M]\{\ddot{u}\} + [C]\{\dot{u}\} + [K]\{u\} = \{F^a\} \qquad (2.2)$$

Where,

$[M]$ = Structural mass matrix

$[C]$ = Structural damping matrix

$[K]$ = Structural stiffness matrix

$\{\ddot{u}\}$ = Nodal acceleration vector

$\{\dot{u}\}$ = Nodal velocity vector

$\{u\}$ = Nodal displacement vector

$\{F^a\}$ = Applied load vector

2.3 Acoustic simulation

2.3.1 Acoustic boundary element method Vs. Acoustic finite element method

1. Acoustic boundary element method (BEM Acoustic)

   Boundary element method reduces complex three dimensional geometry to two-dimensional surface and only discretization of boundary is sufficient in these methods. Basis functions are selected in such way that it should satisfy the governing partial differential equation. Undetermined coefficients are estimated by satisfying the boundary conditions. This method can be used for internal and external sound radiation problems [15].

2. Acoustic finite element method (FEM Acoustic)

   In finite element method [15], acoustic volume is discretized. Basis function is selected in such a way that it should satisfy boundary condition exactly. Undetermined coefficients are determined by satisfying governing partial differential equation.

- Governing equation and boundary condition involved in acoustic analysis are

$$\bigtriangledown^2 p(\overrightarrow{x},t) = \frac{1}{c^2}\frac{\partial^2 p(\overrightarrow{x},t)}{\partial t^2} \tag{2.3}$$

Where, $\bigtriangledown^2 = \frac{\partial^2}{\partial x^2} + \frac{\partial^2}{\partial y^2} + \frac{\partial^2}{\partial z^2}$ for rectangular co-ordinate system

Assuming time is harmonic in nature, acoustic wave equation becomes,
Helmoltz Equtaion

$$\bigtriangledown^2 \bar{p}(\overrightarrow{x}) + k^2 \bar{p}(\overrightarrow{x}) = 0$$
$$p = Re(\bar{p}(\overrightarrow{x})e^{i\omega t})$$

Where, k is wave number and is defined as
$k = \omega/c$

Generally, three types of boundary conditions are used which are normal components of surface velocity, surface pressure, acoustic impedance at the surface.

Surface velocity boundary condition is preferred to apply because it is (i)insensitive to surrounding acoustic field (ii)accurate to measure (iii) easy to predict numerically.

The numerical method used for acoustic analysis is a boundary element method that solves Kirchoff-Helmholtz integral equations with normal surface vibration velocity as boundary conditions. Commercial acoustic software LMS Virtual Lab is used in this study.

2.3.2   Selection of time-step

In dynamic analysis, inertia, stiffness, damping and load plays important role, effect of these factors is captured only when accurate timestep is selected in the analysis. If these factors are not important then static analysis is also sufficient. The accuracy of the transient dynamic solution depends on the integration time step. Smaller time step provides higher accuracy. When time step is too large, then there will be error in calculating higher modes response and overall response of structure. In opposite when time step is too small then solving such system is computationally very expensive. Optimum time step size depend on response frequency of structure. Dynamic response of structure is a combination of all modes, so, it is essential to choose time step such that it should be able to resolve the highest mode that contributes to response. Optimum time step can be chosen based on highest frequency [14], f, as follows,

$$\text{Integration time step} = 1/20f$$

2.4   Selection of field points

The sound field radiated by a source in a free field may be divided into three regions [16]: Hydrodynamic near field, Geometric (or Fresnel) near field, and Far field as shown in Figure. 2.1.

1. Hydrodynamic near field

   The region immediately adjacent to the vibrating surface of the source is considered as the hydrodynamic near field, and this region is dominant upto a distance much less than one wavelength. In this region, the acoustic pressure is out of phase with local particle velocity.

2. Geometric near field

   The geometric near field is next to the hydrodynamic near field. In this region, interference between contributing waves from various parts of the source lead to interference effects and sound pressure levels that do not necessarily decrease monotonically at the rate of 6 dB for each doubling of the distance from the source. Acoustic pressure amplitude in the near field may not give the actual sound power radiated by the source.

3. Far field

   Acoustic pressure and acoustic particle velocity are in phase in far field. In the far field, sound pressure levels decrease monotonically at the rate of 6 dB for each doubling of the distance from the source and the source directivity is well defined. Measurement of sound pressure level in far field is preferred.
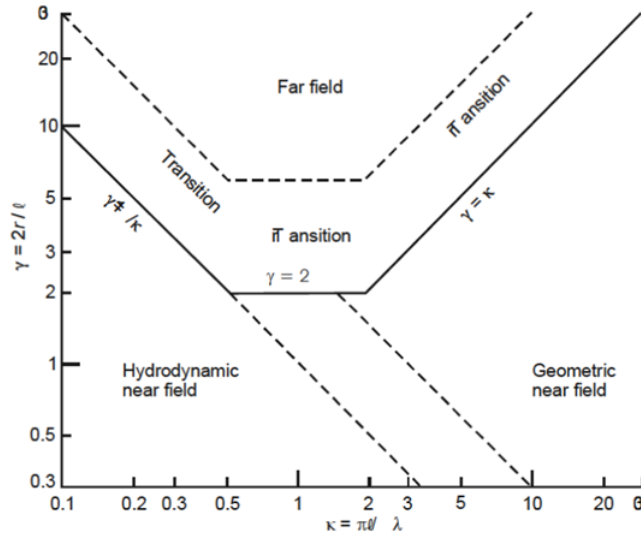
Figure 2.1: Radiation field of source

To charactrise the far field, following three equation need to be satisfied,

$r \gg \lambda/2\pi$, $\qquad$ $r \gg l$, $\qquad$ $r \gg \pi l^2/2\lambda$

Where,

r is the distance from the source to the measurement position,

λ is wavelength of radiated sound,

l is characteristic source dimension.

More generally defining, $\gamma = 2r/l,$ $\qquad$ $\kappa = \pi l/\lambda$
, using these parameters radiation of sound field is classified.

Hitting noise and clonking noise are dominant at 50 Hz to 2000 Hz, so considering this frequency ranges, field point/microphones location is selected in a such way that will satisfy the above three criteria for far field.

2.5 Coupling methods

Coupling equation between fluid and structure can be solved using two approaches [17]

1. Strong Coupling :

   In this approach, to find the solution of coupled problem all governing equation (here for fluid, Navier-stokes equation and for structure, equation of motion)are combined in large system and then solved. At the interface fluid solver and FEM solver solve the equation simultaneously. The solution got from this approach is stable. But solving a system with strong coupling is often difficult as it is computationally expensive.

2. Weak Coupling :

   In this approach, each problem is solved separately and some variables are exchanged and inserted into the equation of other problem. In weak coupling each solver solves the equation until convergence is achieved and then transfers data to other solver. Data can be exchanged in one way or two way coupled approach. This coupling gives less exact solution compared to strong coupling but advantage is that sub-problem can be solved faster than the complete system.

As explained above, exchange of the information between two solvers can take place in two ways one way coupling and two way coupling [18]:

1. One way coupling

   Due to fluid motion, pressure load acts on structure. If the reaction of structure on fluid is negligible then this type of coupling is treated as one way coupling. For this type of problem, as control volume of structure is not changing much, it may be sufficient to use only one way mapping of fluid pressure to the structure.
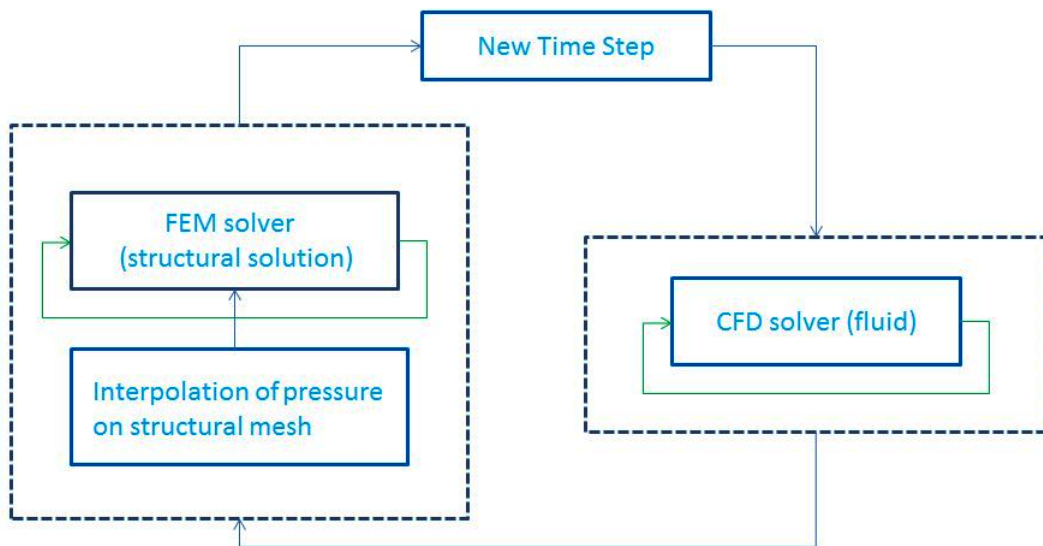
Figure 2.2: Flowchart of one way coupling

Figure. 2.2 explains the one way coupling method. First, CFD solver solves the fluid flow equation until convergence is achieved and then resulting pressure is mapped/interpolated on structural mesh. Structural solver solves structural dynamic equation upto the convergence. The process repeated until the end time is reached.

2. Two way coupling

   Due to fluid motion, pressure load acts on structure. If the control volume of the fluid region changes measurably/significantly then this type of problem needs two way

coupling approach. Generally, for flexible structure (for low modulus of elasticity) two way coupling is preferred.
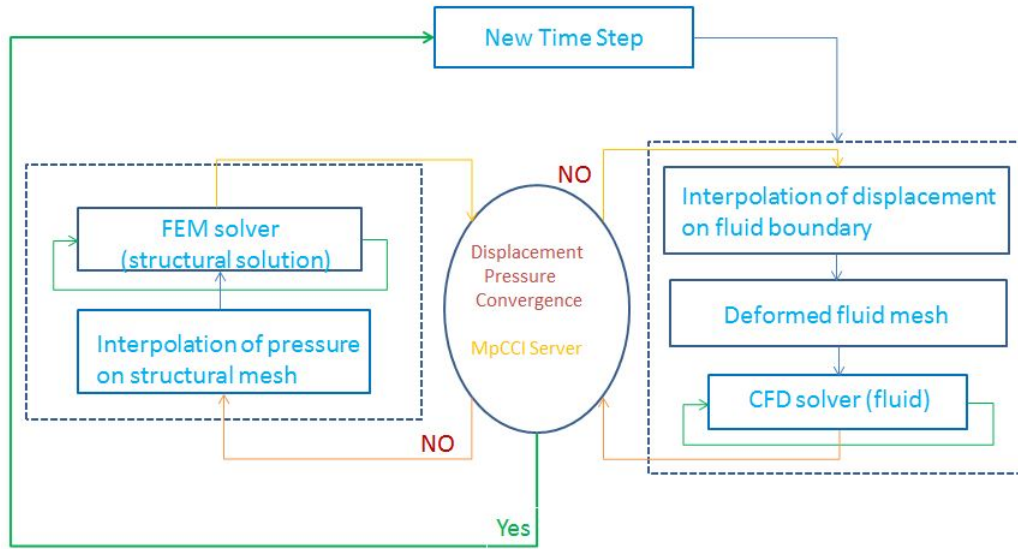
Figure 2.3: Flowchart of two way coupling

Figure. 2.3 shows the flowchart of two way coupled approach. First, Fluid solver solves the fluid flow equation and generated pressure data is mapped/interpolated on structural mesh. In structural dynamic analysis, CFD pressure data is acts as a boundary condition for structural analysis. Deformation from structural solver is mapped on fluid mesh. Both solver solves the equations until convergence is reached, and then it goes to next time step.

Chapter 3

Experimental Setup
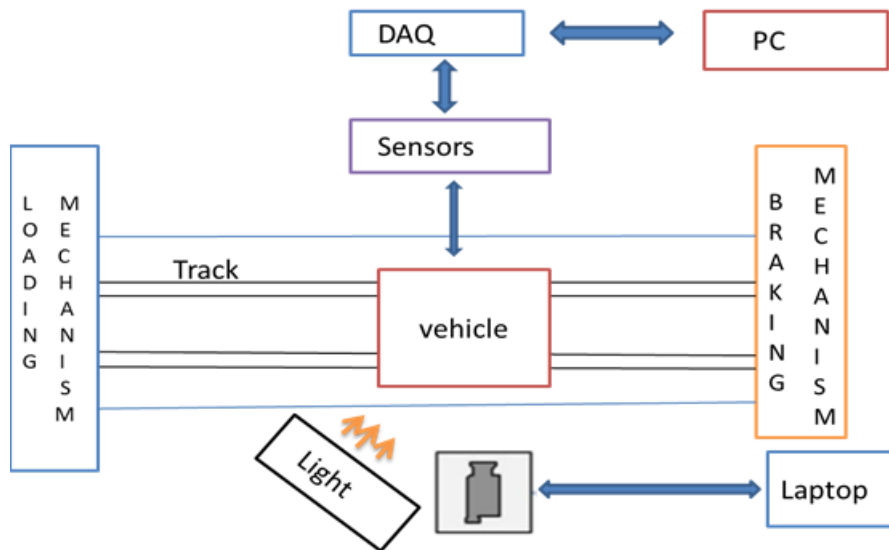
Figure 3.1: Schematic diagram of experimental setup

Figure. 3.1 shows the schematic diagram of the Impact test rig, which simulates the sloshing phenomenon under control braking load to measure dynamic force and dynamic acceleration on the tank wall and also dynamic pressure at the interface of fluid and wall the tank. It also measures sloshing noise radiated from the tank. The system consists of four major subsystems which are loading mechanism, braking mechanism, rectangular tank with provision for sensor mounting and vehicle travel track. The vehicle is accelerated when a dead weight falls due to gravity and the vehicle is attached to the dead weight by a string and pulley mechanism. A band brake is used to apply the brake. The liquid inside the tank sloshes due to the sudden application of the brake.
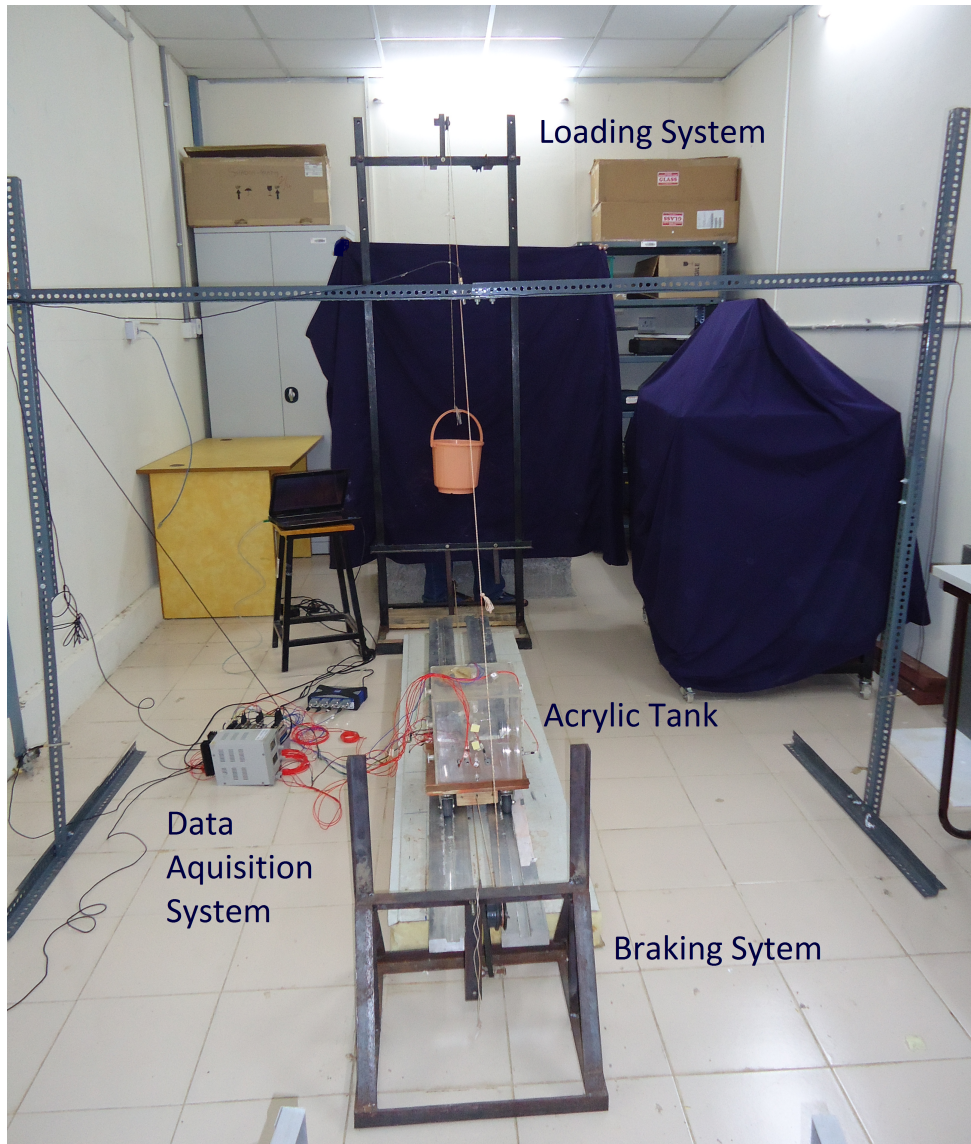
Figure 3.2: Experimental setup

3.1 Subsystem details

1. Loading System

Figure 3.3: Loading System

- Height of dead weight can be varied upto 1.5 m

- dead weights used are 1 kg , 1.2 kg, 2 kg, 3 kg

- mass of dead weight depends upon the acceleration and deceleration needed.

2. Braking System

Figure 3.4: Braking System

- Wheel brakes applied by band brake.

3. Vehicle track System
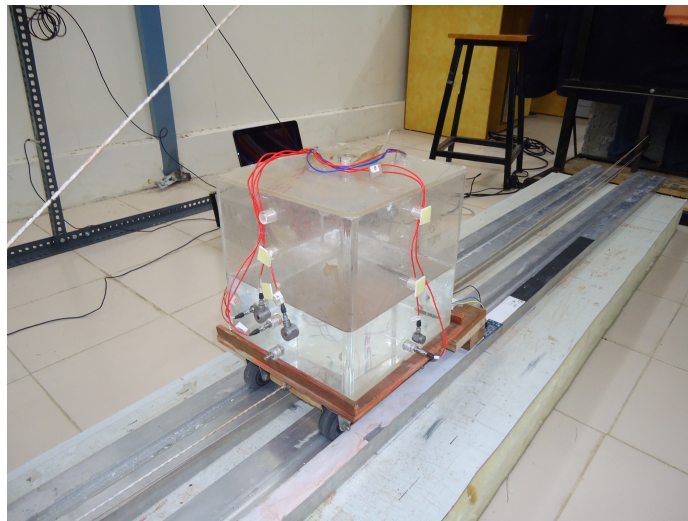
Figure 3.5: Vehicle track system

- An aluminum track of approximately 1.5 m was prepared on which the vehicle would travel. Special care was taken to minimize lateral movement of the vehicle.

4. Rectangular tank with integration of sensors mounting

- Figure. 3.6 shows, A transparent rectangular tank made of Acrylic was fabricated with a length of 238 mm, width of 220 mm and height of 238mm.
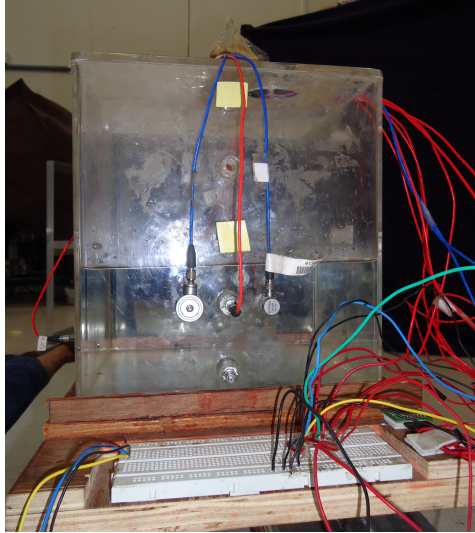
Figure 3.6: Acrylic tank with sensor mountings

- The tank wall was 6 mm thick.

- This tank was placed over a wooden platform that was attached to quieter wheels in order to reduce background noise.

- The platform was maintained at a horizontal position with respect to the ground with the help of a spirit level.

- A three axis linear inertia acceleration sensor (3g-ADXL335) and a line triggering sensor were mounted on this platform. The inertia sensor is used to monitor vehicle acceleration and deceleration.

- Depending on the experimental condition, the sensors can be mounted at 10 %, 30 %, 50 % and 70 % of tank height.

- Figure. 3.7 shows, sensor mounting location for 20 % fill and 60 % fill level. Most of the dynamic action is observed mostly in front and back wall of tank, so dynamic force and dynamic acceleration sensors are mounted on those walls. As fluid comes directly in contact with dynamic pressure sensor, so to capture dynamic events at the wall and fluid interface, dynamic pressure sensors are mounted on front, back and right wall of the tank. As the lateral movement of the tank is avoided, so the same dynamic events can be captured in left and right sensors (so only one dynamic pressure is enough). Sloshing is surface wave phenomenon, to capture this sensor location is fixed at 10 % below fill level. For example, suppose fill level is 60 % then the sensor height should be chosen as 50 % , sensors are also kept at constant 10 % height to see behaviour change at different fluid layers. At each sensor height position, dynamic pressure is mounted at centre and dynamic force and dynamic acceleration sensors are mounted besides to the dynamic pressure sensor.
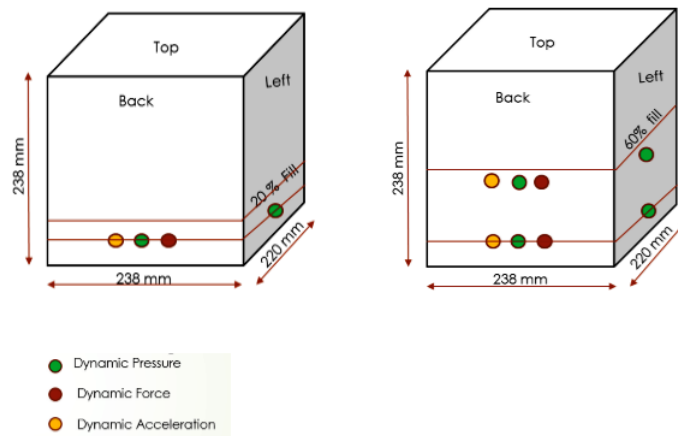
Figure 3.7: Schematic diagram of sensor mounting locations (a) 20 % fill (b) 60 % fill

5. Sensors integration with Data Aquisition
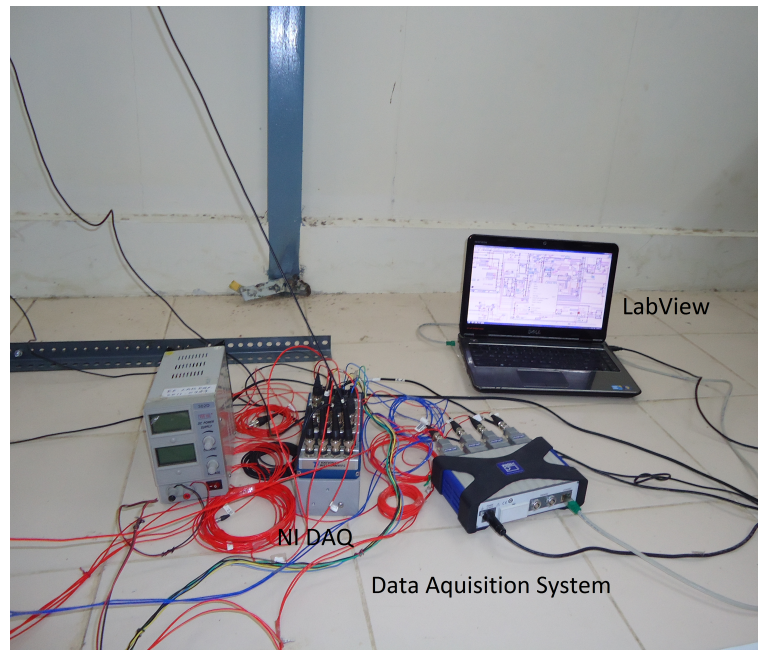
Figure 3.8: Data aquisition setup

- NI cDAQ-9178 data acquisition system

  Figure. 3.9 schematic diagram of DAQ is being used as interface between sensors and LabView software.

  Data from all sensors were acquired using a NI cDAQ-9178 data acquisition system which was triggered by the line sensor, which is in turn was activated by the color change in the vehicle track.

18
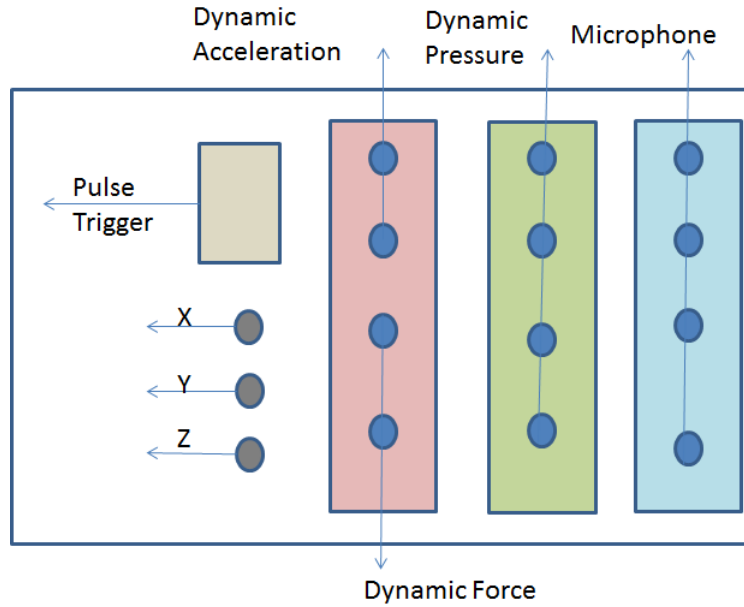
Figure 3.9: Schematic diagram of Data Aquisition system

A customized Labview program was used to acquire the data from all the sensors. Code extended to all the sensors and a way to synchronize the data from these sensors is been established.
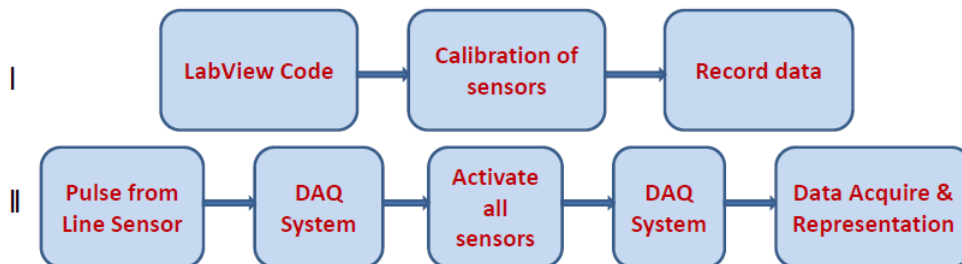
Figure 3.10: Schematic diagram of data aquisition process

- Dynamic force sensors : Figure. 3.11 (a) shows, dynamic force sensor. Dytran 1053V3 and Dytran 1051V4 models used to measure dynamic force on the wall of the tank. Sensitivity of the sensor used was 11.24 mV/N

- Dynamic acceleration sensors Figure 3.11 (b) shows the dynamic acceleration sensor. Dytran 3055B1 with sensitivity 10 mV/g. is used to measure the dynamic acceleration on wall.

- Microphones Figure 3.11 (c) shows the microphone used for experiment. BSWA MPA416 with sensitivity 60 mv/Pa, is used to record the radiated sound pressure

Figure 3.11: Sensors used for data aquisition (a) Dynamic force (b) Dynamic acceleration (c) Microphones (d) High speed camera

level. Four microphone's are kept in front, left, top and right direction.
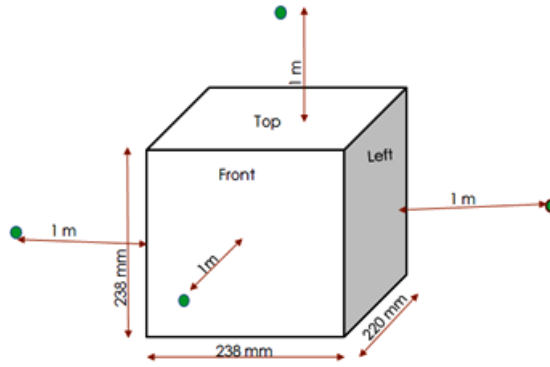
Figure 3.12: Schematic diagram of microphone position

Figure. 3.12 shows To measure sound pressure level accurately, microphone should be kept in far field as shown in Figure 3.12. The distance of far field is selected as per the discussion in section 2.4. By considering interested maximum frequency as 500 Hz, microphone is located at a distance of 1 m from the final resting position of the tank wall.

- High speed camera

  Figure. 3.11 (d) shows high speed camera- Phantom V12.1, used to capture the sloshing events inside the tank. 1000 fps frame rate was used to capture small sloshing moments. Camera is also triggered with rest of the sensors to make it possible to compare all the data with respect to the time frame.

The required acceleration and deceleration are estimated from equations (3.1) and (3.2) respectively,

$$a = \frac{m_2 g - \mu m_1 g}{m_1 + m_2} \tag{3.1}$$

$$d = (\frac{t_1}{t_2})(\frac{m_2 g - \mu m_1 g}{m_1 + m_2}) \tag{3.2}$$

where,

20

m_1 is mass of the tank with water, kg

m_2 is mass of the dead weight, kg

a is acceleration of the tank, m/s^2

d is deceleration of the tank, m/s^2

t_1 is time for acceleration, sec

t_2 is time for deceleration, sec

Depending on the experimental condition, the sensors can be mounted at 10 %, 30 %, 50 % and 70 % of tank height as shown in Figure. 3.7. An extensive study was conducted to determine repeatability of the test data. Parametric studies were conducted with varying fill levels and sensor locations.

Chapter 4

Numerical Analysis

4.1 Fluid Structure Interaction (FSI) coupling

In FSI simulation usually structure deforms due to forces caused by fluid flow. The deformation must be transfered to CFD code which corresponds to quantity nodal position while the pressure and forces are sent from CFD to structural code. MpCCI is a tool to perform multiphysics computations by coupling independent simulation codes. MpCCI (Multi-Physics Code Coupling Interface) is used as coupling tool between CFD solver (STAR-CCM+) and Structural solver (Ansys). MpCCI is a software environment which enables the exchange of data between the meshes of two simulation codes in a multiphysics simulation. MpCCI enables a direct communication between the coupled codes by providing adapters for each code.

4.2 Co-Simulation Methodology

FSI co-simulation follows the following steps [17] :

1. Preparation of Model files:

   Before starting the simulation, model file created in each code i.e. here STAR CCM+ and ANSYS. Model contains definition coupling region and other analysis information.

2. Defining of coupling process:

   After importing the two models in MpCCI environment then the coupling region i.e. specific region which are taking part in actual data transfer in MpCCI are defined. Also the quantities to be transferred are set. For this simulation overpressure data is exchanged from STAR CCM+ to ANSYS and the nodal position data is exchanged from ANSYS to STAR CCM+. Number of time steps, iteration etc. information is defined in coupling process.

3. Running Co-simulation:

After starting the MpCCI server both coupled codes are started. Each code computes its part of the problem while the MpCCI controls the quantity exchange i.e. overpressure and node position.

4. Post processing:

   After the co-simulation, the results are analyzed with the post-processing tools of each simulation code i.e. STAR CCM+ and ANSYS for this case
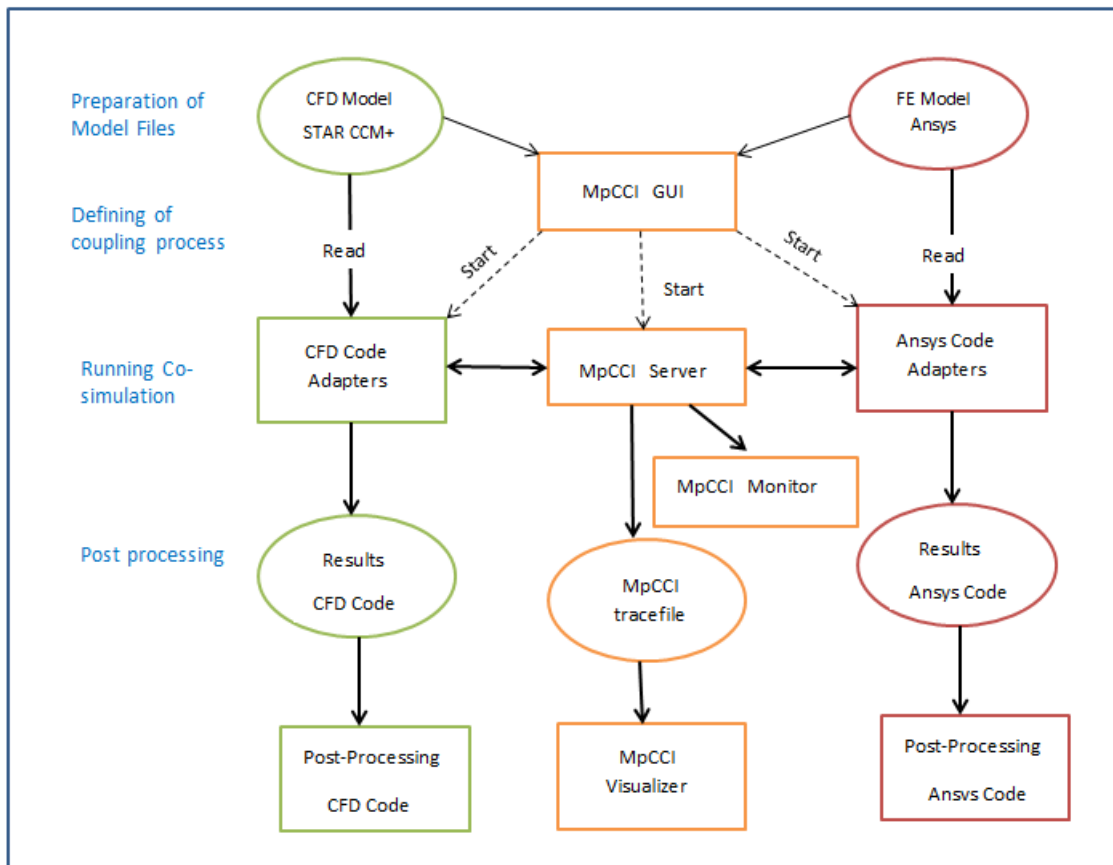
Figure 4.1: Flowchart of co-simulation methodology in MpCCI

4.3 Sloshing Noise prediction methodology

Figure.4.2 shows Sloshing Noise generation mechanism. Based on the structural flexibility of the wall, the problem can be solved either as one-way coupled or two-way coupled FSI problem. This can be used to determine the dynamic pressure and corresponding wall displacement. This vibration displacement acts as a boundary condition in the acoustic analysis. Similarly, in acoustic analysis the tank can be modelled as acoustically rigid or
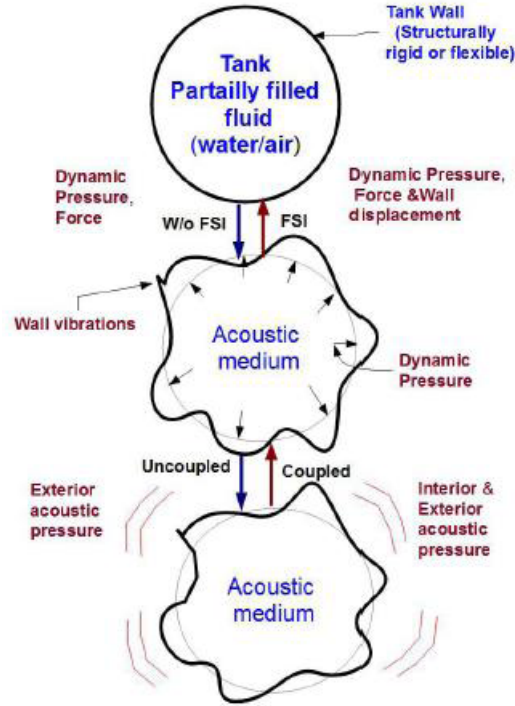
Figure 4.2: Sloshing Noise generation mechanism

flexible. If the tank is acoustically flexible, then it can be modelled as acoustic-structural coupled problem.

4.4 Simulation Methodology of Sloshing Noise

Figure. 4.3 shows the one-way coupled approach for noise generation in time and frequency domain. Displacement in time domain is determined by applying a transient pressure on structural wall. Similarly, using Fast Fourier Transform (FFT) on transient pressure data from CFD, pressure in frequency domain is determined. It is applied as excitation to the structural wall and corresponding harmonic displacement is calculated by doing harmonic FEM analysis. These displacements are used as acoustic boundary conditions in corresponding acoustic transient FEM and acoustic harmonic BEM analysis. Propagating sound pressure level is determined at defined field point locations.

As mentioned before, noise generated due to liquid sloshing is categorized into three types of noise sources, which are Clonk, Hit and Splash Noise. Clonk and Hit noise dominates the frequency range of 50 Hz to 2000 Hz and Splash noise is dominants in the higher frequency range of 500 Hz to 10 kHz range. The splash noise is due to the liquid-liquid interaction.The current proposed Vibro-acoustic model will not compute splash noise.

The frequency domain approach can be performed by taking pressure loading on tank
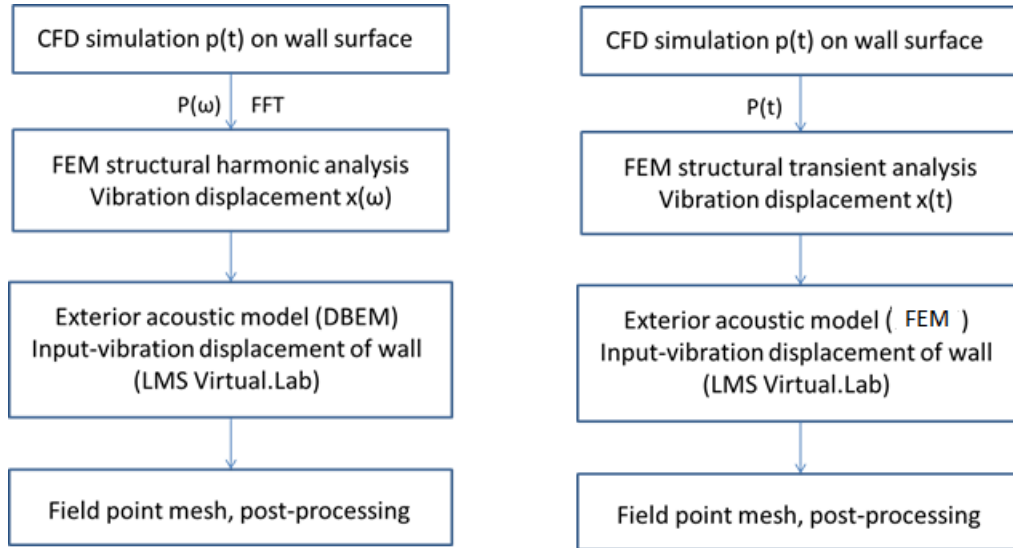
Figure 4.3: Tank sloshing simulation methodology

walls from computational fluid dynamics (CFD) study. This approach is valid for linear sloshing regime where it is assumed that the change in the liquid center of gravity is negligible. However, it may not be true for higher deceleration loading. Hence, it is required to consider a time domain approach for nonlinear sloshing. Nonlinear sloshing predominates for higher deceleration loading or higher fill levels. The current analysis assumes that the tank walls are acoustically rigid and therefore one-way coupling was considered.

4.5 Structural Simulation

Modal analysis is performed in order to demonstrate the contribution of the structural properties of the tank in the slosh noise prediction. In this part of the present investigation the linear isotropic material (Acrylic) is used. Shell 63 element used to mesh the wall surface area and there are 29,000 shell elements as shown in Fugure. 4.4 for the fuel tank. Following material properties is used for structural analysis, modulus of elasticity 2.1e9 N/m^2, poissons ratio is 0.4 and density 1100 kg/m^2.

Acoustic boundary element model of tank volume has to be created. The acoustic boundary element size is determined by the wavelength of the highest frequency interest. At least six elements per wave length are required for the simulation [15]. Assuming that the sound is traveling through air at standard temperature and density, Table 4.1 shows the highest frequency and the recommended element size for the simulation.
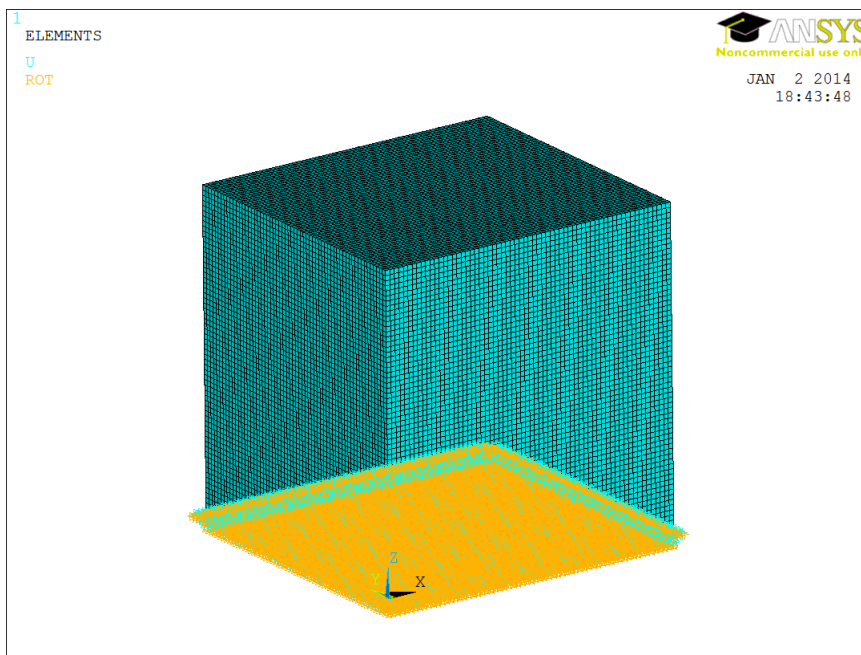
Figure 4.4: Structural analysis model

Table 4.1: Maximum frequency and recommanded element size

Maximum Frequency(Hz)	Recommanded element size(mm)
500	113
1000	57
1500	38
2000	28
2500	23
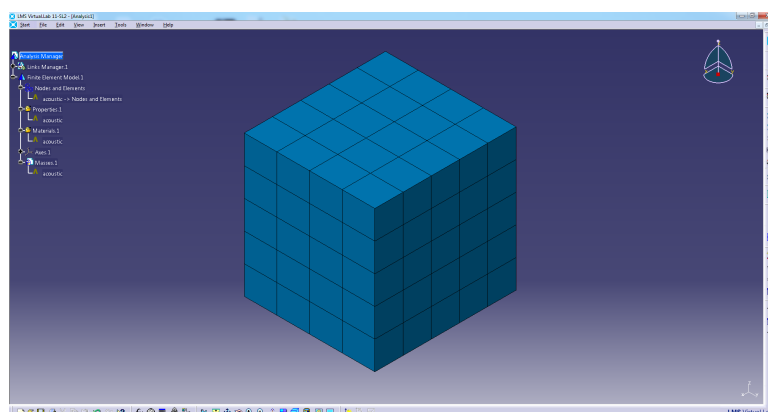
Figure 4.5: Acoustic analysis model

Chapter 5

Results and discussion

5.1 Experimental Analysis

Following conditions and assumptions are considered through out the experiment.

1. Starting point of the vehicle is always fixed.

2. All sensors are triggered from the same point of location i.e. 0.65 m from the starting point, and the application of brake takes place at 0.25 m distance from triggered location.

3. Effect of string elasticity is not considered.

4. Microphone locations are fixed at 1m distance from each of the side wall and top wall of tank.

5.1.1 Parametric Study

Following parametric studies have been conducted to understand the sloshing behavior at different fill level and deceleration level.

1. Fill Level : 20 %

   Sensor Height : 10 % of fill level

   Deceleration : 0.2 g , 0.25 g , 0.3 g

2. Fill Level: 40 %

   Sensor Height : 10 % and 30 % of fill level

   Deceleration :0.2 g , 0.25 g , 0.3 g

3. Fill Level : 60 %

    Sensor Height : 10 % and 50 % of fill level

    Deceleration : 0.2 g , 0.25 g ,0.3 g

4. Fill Level: 80 %

    Sensor Height : 10 % and 70 % of fill level

    Deceleration : 0.25 g

5.1.2 Estimation of background noise
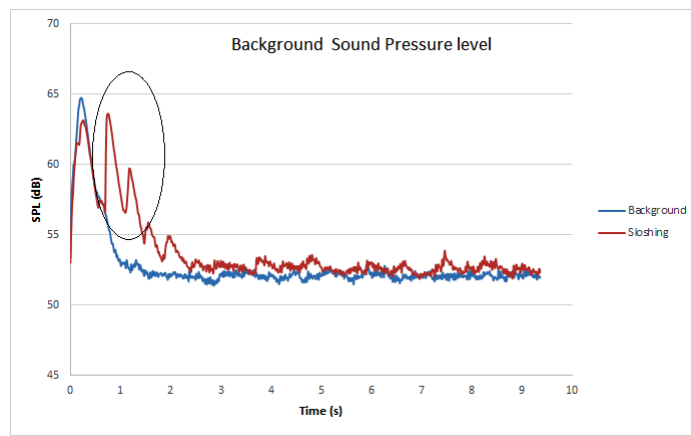
Figure 5.1: Background noise radiated from tank filled with (a) water (b) sand

Before starting the experiment it is important to estimate background noise. Test is carried out in two cases to see the effective sloshing region. In first case, tank is filled with water and run on ITS setup , and corresponding sloshing noise is recorded. While in second case water in tank is replaced with equal weight of sand and the system is ran to record corresponding noise. From Figure. 5.1, it is observed that vehicle background noise before braking is captured in both cases, but after braking sloshing noise is dominant. So, in following experimental parametric studies the first spl peak is corresponding to background noise which includes friction of tires with track,thread-pulley noise etc.

5.1.3 Different regimes in sloshing

Figure. 5.2 shows, different regimes in sloshing.

After sudden braking, fluid inside the tank sloshes. The sloshing behavior of fluid inside the tank is different for different fill level, and different deceleration level. Sloshing behavior inside tank can be classified in to three regimes which are Impact regime (Non-linear), transition regime (weakly nonlinear) and linear regime.

28
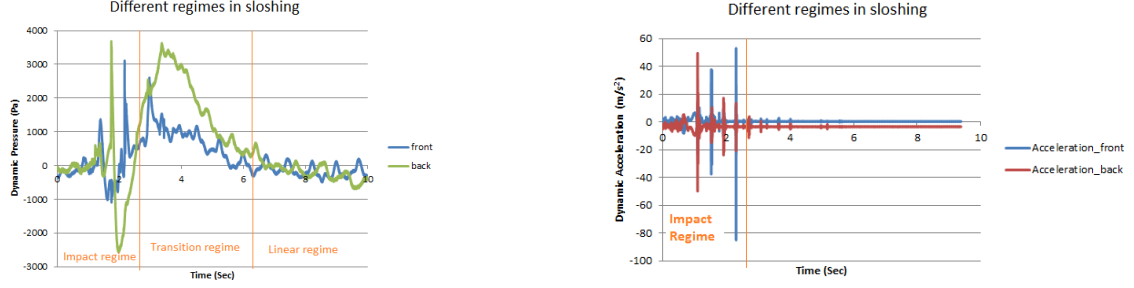
Figure 5.2: Different sloshing regimes in sloshing (a) Dynamic pressure (b) Dynamic acceleration

1. Linear Regime : This regime is charactrised by, small oscillations in which the fluid free surface remains planar without rotation.

2. Weakly nonlinear : This regime is charactrised by, relatively-large-amplitude oscillations in which the free liquid surface experiences nonplanar motion. This regime is described by a differential equation with weak nonlinearity.

3. Nonlinear Regime : This regime is charactrised by, strongly nonlinear motion where the nonlinearity is mainly due to rapid velocity changes associated with hydrodynamic pressure impacts of the liquid motion close to the free surface.

After braking, the sloshing waves with certain velocity strikes on tank walls and momentum of sloshing waves is converted into vibration of tank wall. Major portion of wave energy is lost in this regime. The impact phenomenon is captured in all sensors viz. Dynamic prssure, Dynamic acceleration, Dynamic force and the corresponding impact noise is also captured by microphone. Effectiveness in simulation can be achieved, if the simulation is run for impact regime time duration. Next to the impact regime, there is transition regime, it lies between sloshing linear regime and impact regime. After hitting, fluid takes some time to reach linear planar motion and this time duration regime is charactrised by transition zone. In this regime, mostly bubbly pattern near the wall interface is observed. After completion of transition regime, fluid inside the tank sloshes in planar motion. In this regime, pressure sensor senses the fluid pressure due to wave motion inside the tank but wave doesn't have enough energy to produce vibration. Sloshing natural frequency is clearly observed in this regime.

5.1.4 Critical sloshing period for numerical simulation

Sloshing behaviour is different, for different fill level and for deceleration. Here, Critical time is defined as, the duration of time upto which hitting event in sloshing. This time corresponding to the impact region as defined in section 5.1.3.
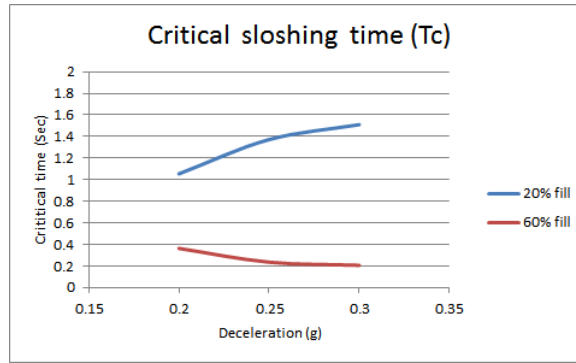
Figure 5.3: Effect of fill level and deceleration level on critical time

The main difficulties while solving FSI transient problem is, duration of simulation and size of result file. Sloshing phenomenon is a transient event, and only impact region is important to find out wall displacement. Optimation in simulation is achieved by running the simulation only for critical time duration. From the experiment data, sloshing event are classified in to impact, transition, and linear regime.

Figure.5.3 shows critical sloshing time variation with different deceleration and different fill level. For 20 % fill level, modal (sloshing) fluid mass is more as compared to rigid mass, so, all fluid takes part in sloshing phenomenon. For 20 % fill, fluid occupies less portion of total volume of tank and will get more surface area for hitting to the front and back wall. As the deceleration level increases, fluid sloshes with high velocity and impacts back and front wall, which continues for two cycles. So, it is important to run FSI simulation upto these cycles. After this region sloshing doesn't play any active role on structure.

For 60 % fill level, modal (sloshing) mass is less compared to rigid mass in the tank. Due to large inertia system reaches linear regime in very less duration of time. From Figure. 5.3, it is clear that as the deceleration level increases the critical time (impact duration) decreases. At higher fill levels water gets less area of back wall to hit and water climbs over back wall and hits the top wall. At higher deceleration, fluid sloshes in highly non-linear manner and mostly splashing is observed.

5.1.5 Experimental result analysis

1. 20 % fill level - deceleration 0.2 g - Sensor height 10%

Figure 5.4: Experimental results for 20 % fill and 0.2 g deceleration case(a) Inertial acceleration (b) Dynamic acceleration (c) SPL (d) Dynamic Force (e) Dynamic pressure (f) Linear regime in sloshing

Experiment has been carried out for 20 % fill level, deceleration 0.2 g and sensor height 10% of the tank height. The required deceleration is obtained based on appropriate dead load selection. Figure. 5.4 shows the recorded test data of tri-axial inertial acceleration data, dynamic force and dynamic acceleration due to wall vibration, and radiated sound pressure level, dynamic pressure due to fluid impact and sloshing linear regime.

In the inertial acceleration data, it is seen that there is application of brake that takes place at 0.99 sec and corresponding fluid motion inside the tank is shown in Figure. 5.5 (a) as event 1. In this instant, the water rises over the front wall. This movement of fluid has been sensed by front pressure sensor as it gives a peak at time of brake application. After brake application, the vehicle moves some distance in reverse direction due to elasticity of string used for brake application. Background

31
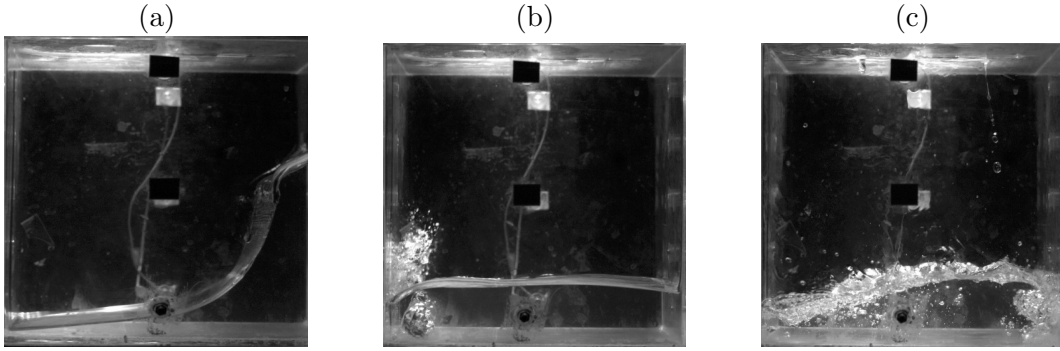
Figure 5.5: 20 % fill, 0.2 g sloshing events(a) event 1 (b) event 2 (c) event 3

noise related to vehicle motion is captured before first peak in SPL. Application of brake takes place at 0.99 sec and is continue for 0.5 sec. This event is shown in inertial acceration data of Figure.5.4 (a).

Dynamic force and dynamic acceleration plots shows that the first event occurs at the back wall which is followed by the second event at the front wall. The fluid moves towards the back wall thereby making a tremendous impact on the back wall at 1.10 sec, this event has been captured in all the four dynamic sensors. This impact at back wall is recorded as non-linear sloshing event in high speed camera image as shown in Figure 5.5 (b), where the fluid hits the wall non-linearely. A part of this fluid has climbed upon the back wall thereby hitting the top surface. After fluid hits on back wall, corresponding sound pressure level peak is recorded at 0.04 sec after hitting event on force sensor. Second impact is captured on the front wall as shown in Figure. 5.5 (c) and noted as event 3, relatively smaller amplitude than event 1 and event 2 and corresponding SPL is recorded. The peak response of the dynamic force in front and back direction is out of phase. It is observed from the high speed camera images that due to forward motion of the fluid after the application of brake, the liquid recedes from the back wall. Therefore when a peak in the dynamic force is observed at the front wall, a trough is noted at the back wall. Similarly, when the liquid sloshes towards the back wall, there is a rise in the dynamic force at the back wall with a corresponding decrease at the front wall. The dynamic force response and tank wall accelerations are related and the trend is similar.

After completion of impact regime/phenomenon, there is transition state where too much bubbly flow is observed and fluid tries to settle down and reach to linear regime. In linear regime, water oscillates in planar motion and sloshing natural frequency is captured. Linear regime fluid doesn't have enough energy to convert available energy to vibrations.

2. 20% fill level - deceleration 0.25 g - Sensor height 10%
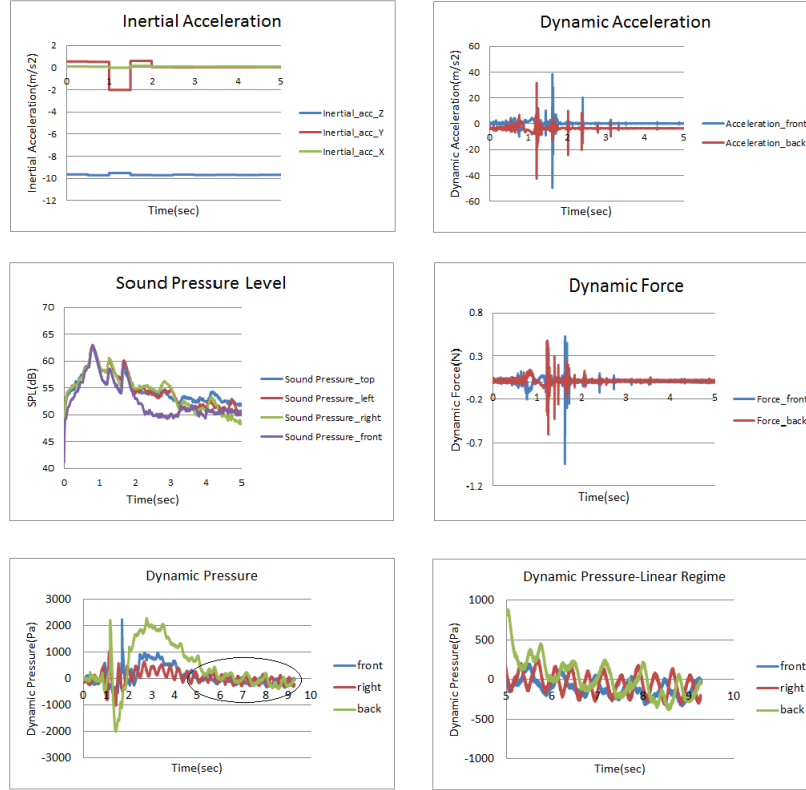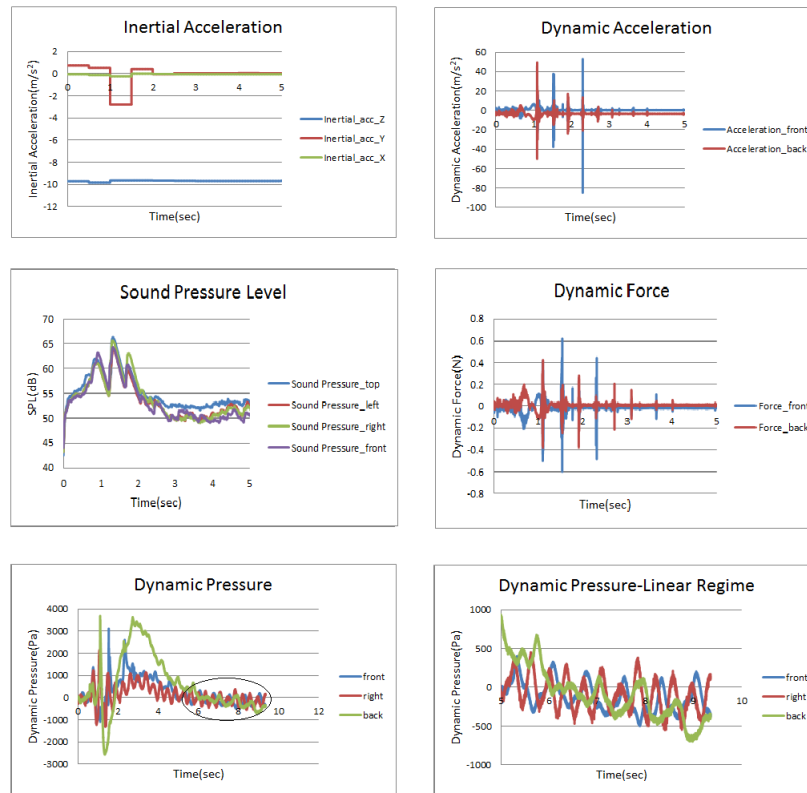

Figure 5.6: Experimental results for 20 % fill and 0.25 g deceleration case(a) Inertial acceleration (b) Dynamic acceleration (c) Dynamic Force (d) SPL (e) Dynamic pressure (f) Linear regime in sloshing

Experiment has been performed for 20 % fill level,deceleration 0.25 g and sensor height 10% of the tank height. The required deceleration is obtained based on appropriate dead load selection. Figure.5.6 shows the recorded test data of tri-axial inertial acceleration data, dynamic force and dynamic acceleration due to wall vibration, radiated sound pressure level, dynamic pressure due to fluid impact and sloshing linear regime.

The condition of fluid inside the tank at the time of brake application (0.99 sec) is as shown in Figure. 5.7 (a), it is observed that most part of fluid has already moved towards the front wall and climbed on the walls. Upto 0.99 sec, the noise captured by microphone is background noise due to vehicle motion. After braking, effective sloshing noise is captured. There is application of brake at 0.99 sec and it continues for 0.5 sec. After that fluid starts moving towards back wall and hits on it at 1.103 sec, as shown in Figure. 5.7 (b). But, most of the water moves on the wall and hits the top wall of the tank after 0.05 sec of hitting on back wall. First back peak is captured by dynamic force sensor and dynamic acceleration sensor but at this instant microphone shows little event but the major hitting occurs on top wall. Corresponding top microphone also shows large SPL peak . Constant time lag between microphone
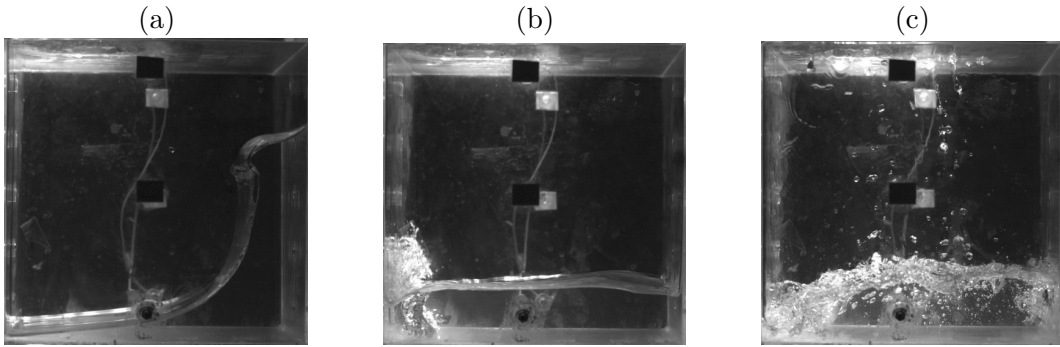
Figure 5.7: 20 % fill, 0.25 g sloshing events(a) event 1 (b) event 2 (c) event 3

data and force/acceleration data is observed i.e. 0.03 sec. Wave front then hits to the front wall at 1.54 sec, as shown in Figure. 5.7 (c). There is scope to keep sensors on the top surface also to capture sloshing events at high deceleration and high fill level. Impact regime continues for two cycles and after there is transition to next regime. To reach in linear regime, it takes slightly higher time than 0.2 g deceleration case. After coming in linear regime, sloshing natural frequency is determined and validated with analytical sloshing natural frequency.

3. 20% fill level - deceleration 0.3 g - Sensor height 10%
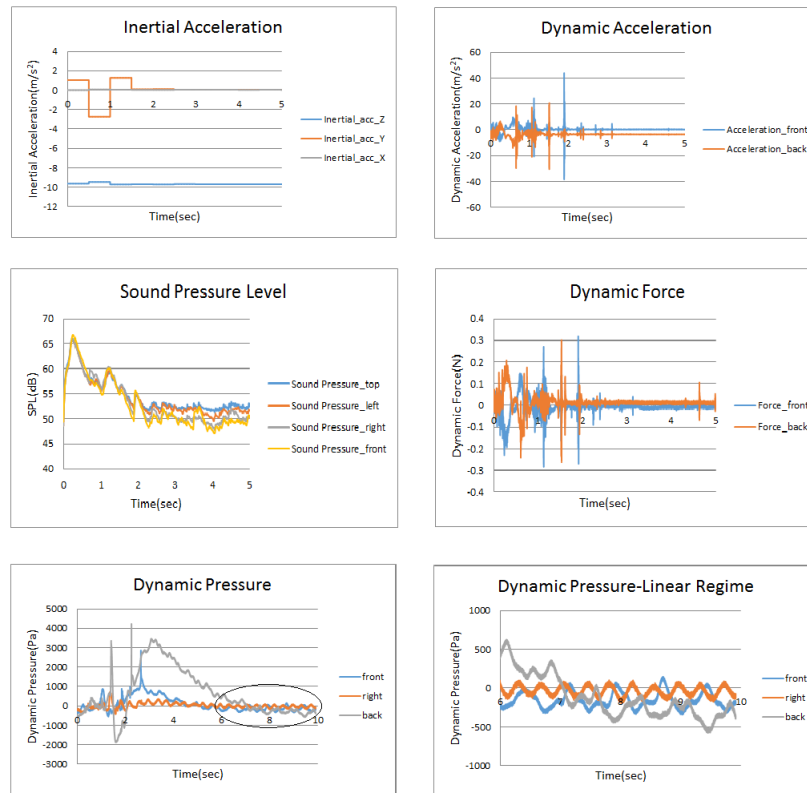
Figure 5.8: Experimental results for 20 % fill and 0.3 g deceleration case(a) Inertial acceleration (b) Dynamic acceleration (c) SPL (d) Dynamic Force (e) Dynamic pressure (f) Linear regime in sloshing

Experiment has been performed for 20 % fill level, deceleration 0.3 g and sensor height 10% of the tank height. The required deceleration is obtained based on appropriate dead load selection. Figure. 5.8 shows the recorded test data of tri-axial inertial acceleration data, dynamic force and dynamic acceleration due to wall vibration, radiated sound pressure level, dynamic pressure due to fluid impact and sloshing linear regime.

Application of brake is takes place at 0.499 sec and continues for 0.5 sec . Figure. 5.9 (a) shows high speed camera image of the starting of braking event and from this image it is clear that water rises on front wall. As the brake applied the fluid with high velocity hits on the back wall and simultaneously on top wall. Dynamic force, dynamic acceleration shows peak correponding to the wall displacent. SPL data for first hit as shown in Figure. 5.9 (b) which is small in amplitude after that high velocity fluid impacted on top wall and major hitting noise is captured by microphone. Microphone is showing peak after some timelag of back force data i.e back side hitting instant. After completion of back hitting event, fluid moves towards front wall and hits as shown in Figure. 5.9 (c) and corresponding dynamic event captured in all sensor mounted on

35
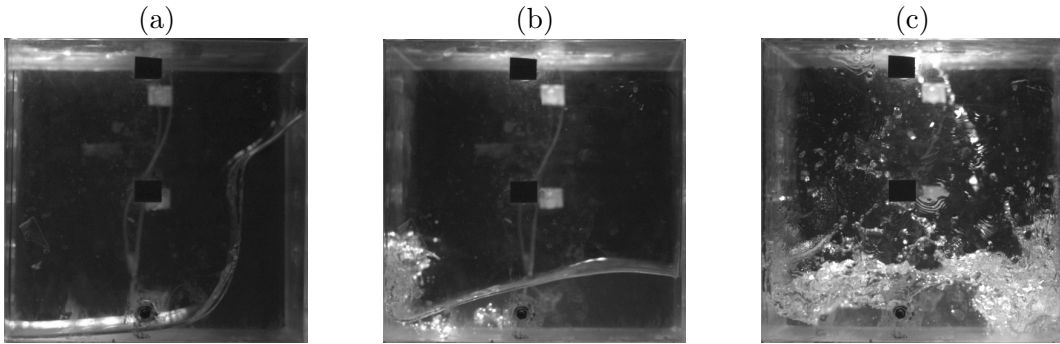
Figure 5.9: 20 % fill, 0.3 g sloshing events(a) event 1 (b) event 2 (c) event 3

front wall. SPL peak in between of hitting event that corresponds to splashing noise (liquid-liquid interaction) is also captured in micrphone data. At the splasing events, no major activity is captured in force and acceleration data, means no vibration event is captured at this instant. Splashing behavior is confirmed by observing fluid motion inside the tank with the help of high speed camera . As the deceleration level is very high, hence too much nonlinearity in sloshing is observed. Sloshing continues for two cycles. Compared to above two cases, for this case fluid takes more time to reach linear. Experimental sloshing period is verified with theoretical sloshing period in linear regime.

4. 40% fill level - deceleration 0.2 g - Sensor height 10% and 30%
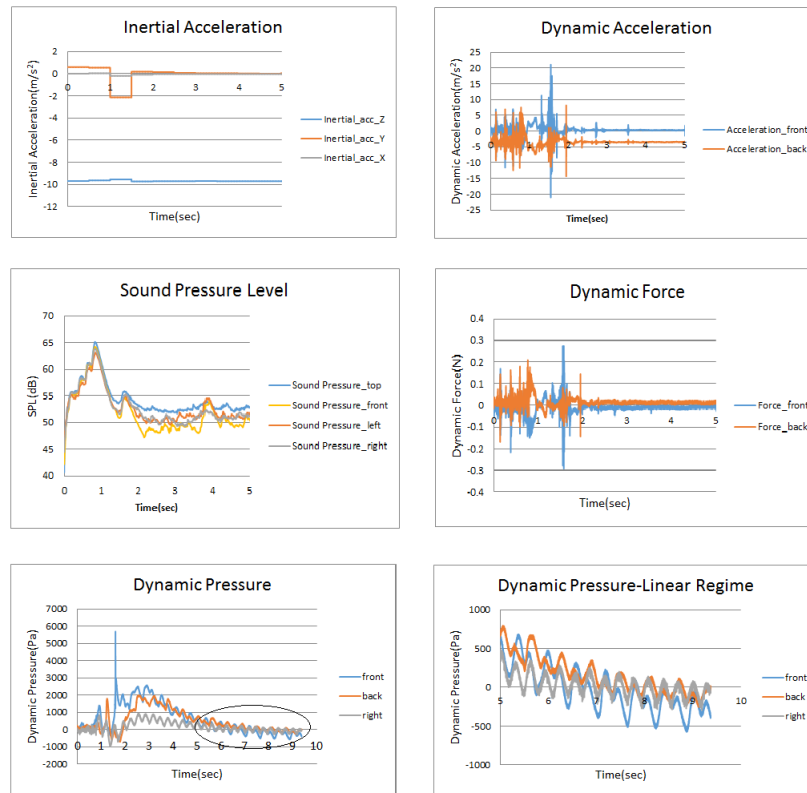
Figure 5.10: Experimental results for 40 % fill and 0.2 g deceleration case(a) Inertial acceleration (b) Dynamic acceleration (c) SPL (d) Dynamic Force (e) Dynamic pressure (f) Linear regime in sloshing

Experiment has been performed for 40 % fill level, deceleration 0.2 g, sensor height at 10% and 30% of the tank height. Sensor height is varied to analyse effect of sloshing behavior at different tank height. The required deceleration is obtained based on appropriate dead load selection. Figure. 5.10 shows the recorded test data of tri-axial inertial acceleration data, dynamic force, dynamic acceleration due to wall vibration, radiated sound pressure level, dynamic pressure due to fluid impact and sloshing linear regime.

As the vehicle moves in forward direction, fluid rises over front wall. Figure 5.11 (a) shows the condition of fluid at the time of braking. SPL data shows first peak before brake is applied and that is corresponding to vehicle background noise. After braking, the wave front doesn't hit to the back wall directly, fluid rises on back wall and hits to the top wall as shown in Figure. 5.11 (b). After this major impact is observed on front wall and corresponding peaks in dynamic force, dynamic acceleration and dynamic pressure is observed. Microphone has captured the corresponding noise as SPL peak, and it has strong correlation with force and acceleration. So, corresponding noise is referred as hitting noise. After this event, no major events captured in force and
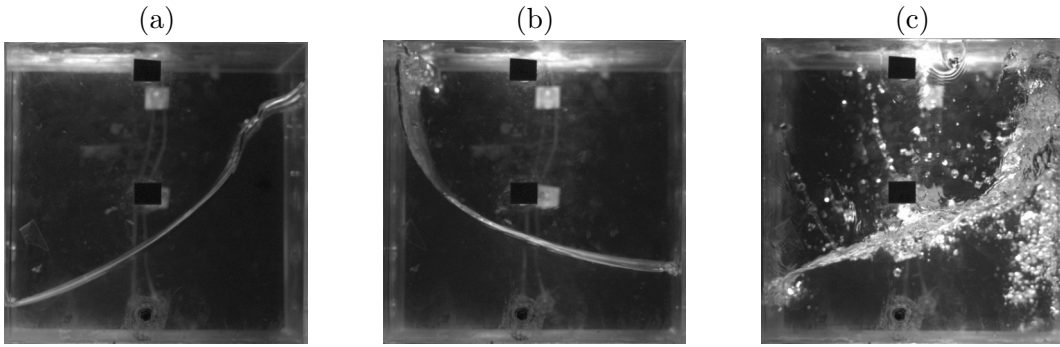
Figure 5.11: 40 % fill, 0.2 g sloshing events(a) event 1 (b) event 2 (c) event 3

acceleration but with the help of high speed camera images fluid splashing is observed. As the sloshing is surface wave phenomenon, So the top layers plays the important role in sloshing. In tank fluid sloshing, fluid is classified into, two parts first part is rigid mass and second part is modal mass. First part is directly proportional to the acceleration of tank and is caused as fluid moves in unison with the tank. Second part, convective part, caused by free surface motion of the fluid inside the tank.

For 40 % fill case, experiment is performed at two different sensor height i.e. 10 % and 30 % as shown in Figure 5.12. By comparing these two cases, it is observed that most of the dynamic events are captured in sensors that are kept at 30% height. There is significant difference in magnitude of dynamic force, dynamic acceleration and dynamic pressure between these two cases. Placing sensor below 10 % of of fill level is not useful to capture dynamic pressure. Dynamic acceleration and dynamic force data senses the wall vibration so force and acceleration sensor at 10 % height can show dynamic event in phase with sensor at 30 % height and difference in magnitude is also slight. Sound pressure level is independent of sensor height so this is not considered for sensor mounting effect.
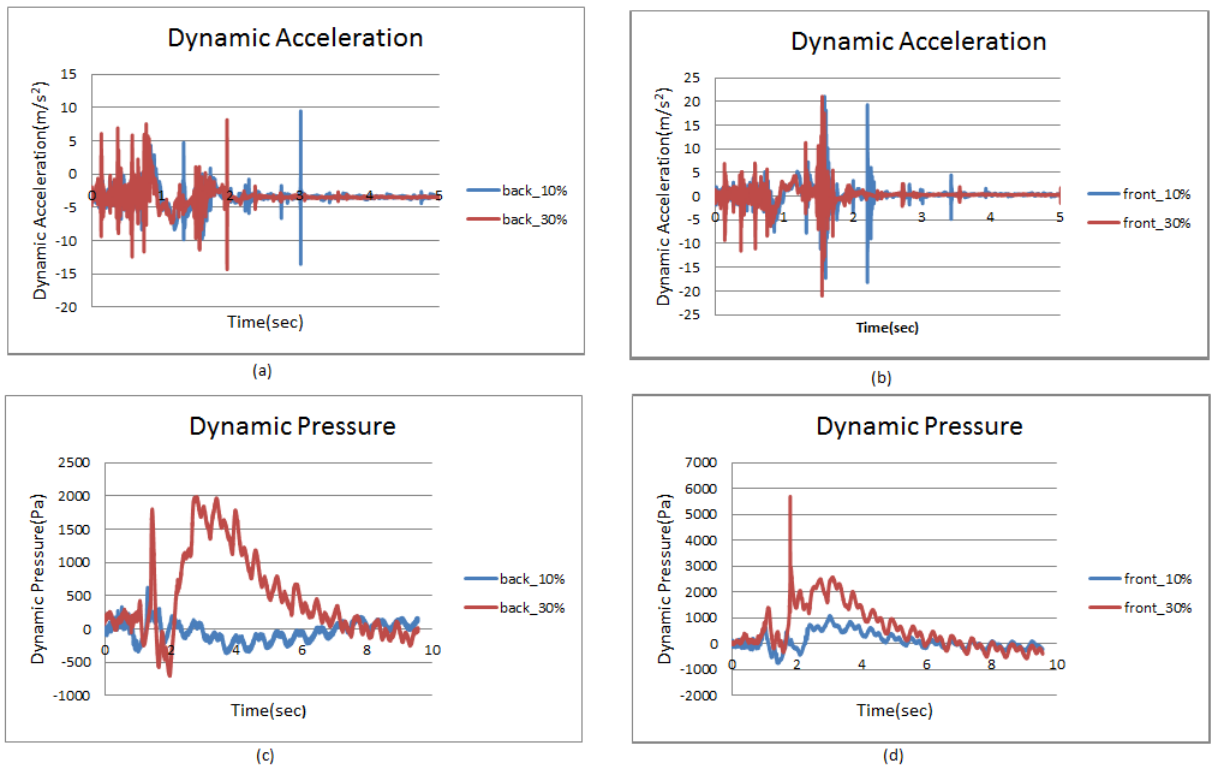
Figure 5.12: Comparison of sloshing behavior for 40% fill level, 0.2 g deceleration and at sensor height 10 % and 30 % (a) Backside dynamic acceleration (b) Frontside dynamic acceleration (c) Backside dynamic pressure (d) Frontside dynamic pressure

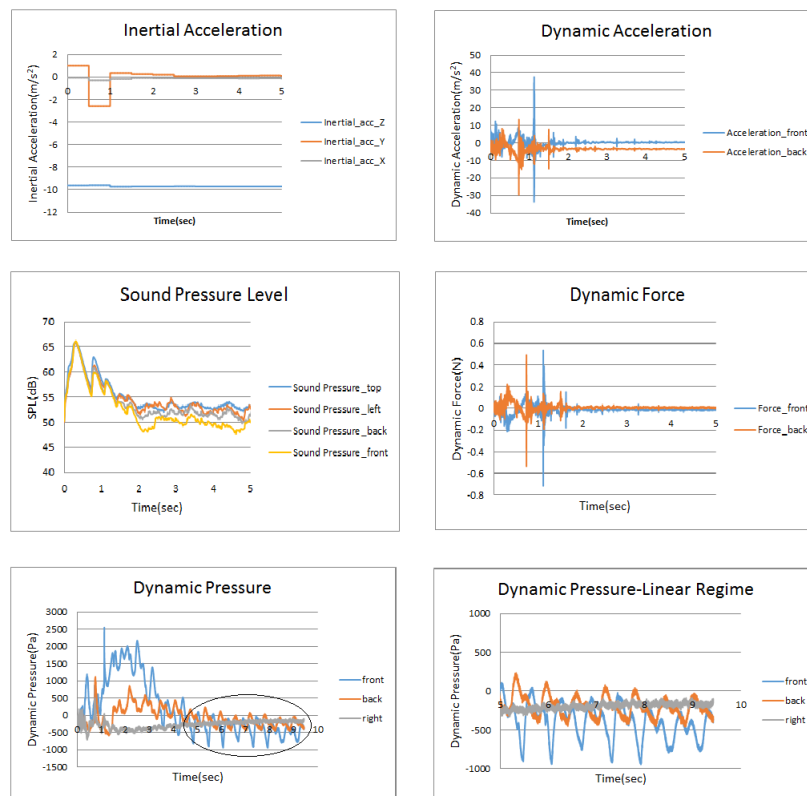5. 40% fill level - deceleration 0.25 g - Sensor height 10% and 30%

Figure 5.13: Experimental results for 40 % fill and 0.25 g deceleration case (a) Inertial acceleration (b) Dynamic acceleration (c) SPL (d) Dynamic Force (e) Dynamic pressure (f) Linear regime in sloshing

Experiment has been performed for 40 % fill level, deceleration 0.25 g and sensor height at 30% of the tank height. Sensor height is varied to analyse effect of sloshing behavior at different tank height. The required deceleration is obtained based on appropriate dead load selection. Figure. 5.13 shows the recorded test data of tri-axial inertial acceleration data, dynamic force, dynamic acceleration due to wall vibration, dynamic pressure due to fluid impact, and radiated sound pressure level.

As the vehicle moves in forward direction fluid moves over front wall. Figure 5.14 (a) shows the condition of fluid at the time of braking and at this stage fluid stores its energy in the form of potential energy. SPL data shows peak between starting point vehicle and starting point of braking instant that corresponding to vehicle motion noise (tyre noise, pulley etc.). After braking, the fluid hits the back wall, and at this instant dynamic force, dynamic acceleration and dynamic pressure have peaks. After that the fluid hits the top wall as shown in Figure. 5.14 (b). At this point, sound pressue is gives first peak . After this event, major impact is observed on front wall as shown in Figure 5.14 (c) and corresponding peaks in dynamic force , dynamic acceleration and dynamic pressure is observed . Microphone has captured the corresponding noise as
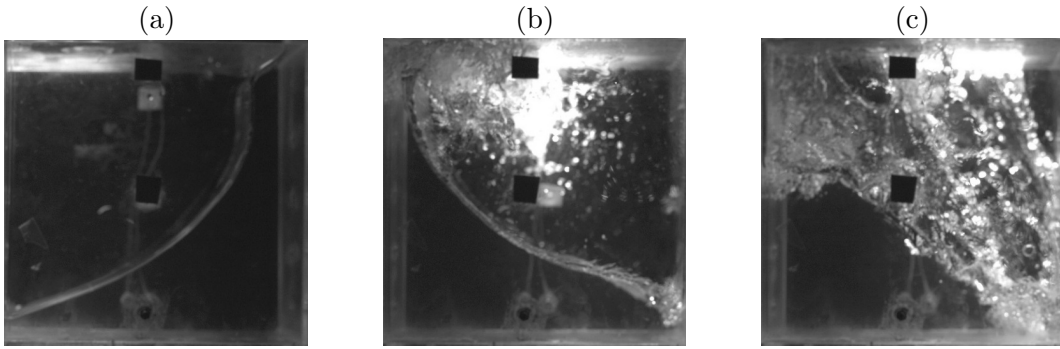
40

Figure 5.14: 40 % fill, 0.25 g sloshing events (a) event 1 (b) event 2 (c) event 3

SPL peak. It has strong correlation with force and acceleration so corresponding noise is referred as hitting noise. After this event, no major events captured in force and acceleration. Dynamic pressure sensor senses the fluid motion for complete duration of sloshing incluiding linear sloshing. Complete sloshing event duration is less in 40 % fill level compared to 20 % fill level. After coming into the linear regime, fluid sloshes in planar up-down motion and sloshing period calculated in this region. This matches with the theoretical sloshing period hence current setup is able to capture sloshing phenomenon.

As the sloshing is surface wave phenomenon, the top layers plays an important role in sloshing. In tank fluid sloshing, fluid mass is classified into two parts, first part is rigid mass and second part, is modal mass or sloshing mass. First part is directly proportional to the acceleration of tank. This is caused as fluid moves in unison with the tank. Second part is convective part, caused by free surface motion of the fluid inside the tank. Similar behavior is observed for 20 % fill level. For 40 % fill case, experiment is performed at two different sensor height i.e. 10 % and 30 %.

By comparing these two cases, it is observed that most of the dynamic events are captured in sensors which are kept at 30% height than 10% sensor height. There is difference in magnitude of dynamic force, dynamic acceleration and dynamic pressure between these two cases. Sound pressure level is independent of sensor height.
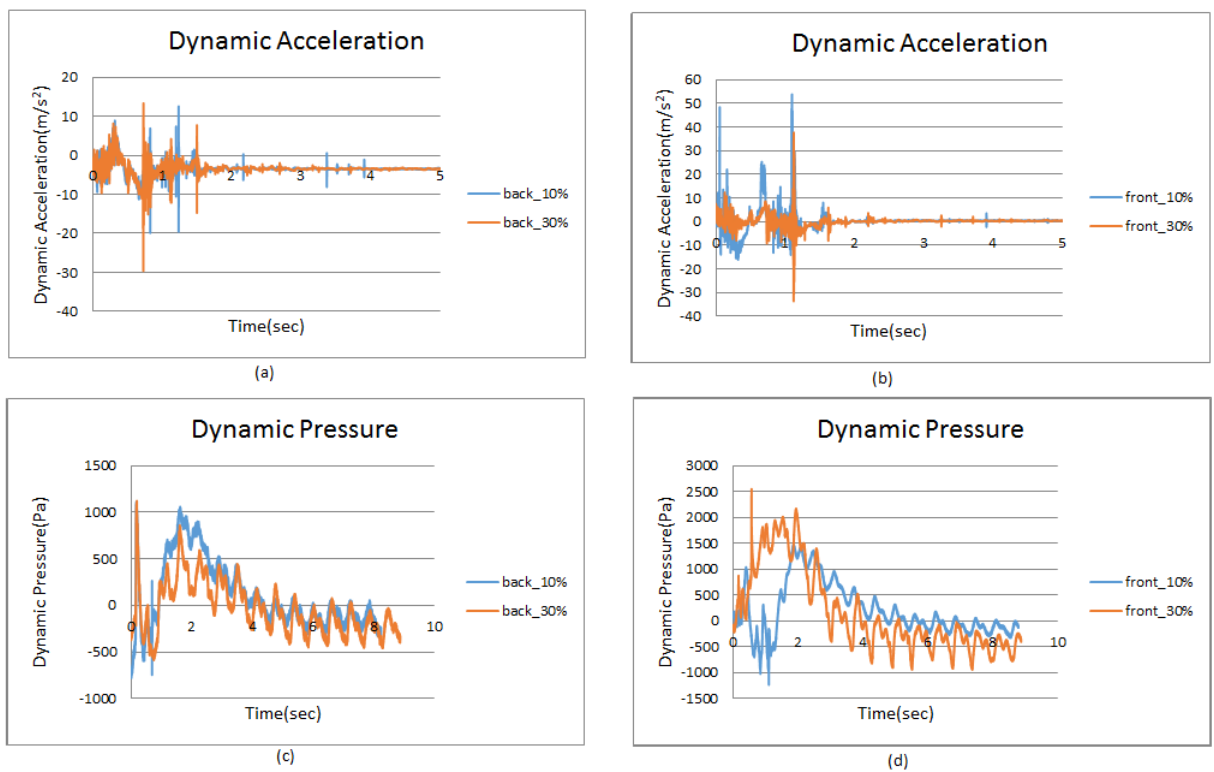
Figure 5.15: Comparison of sloshing behavior for 40% fill level, 0.25 g deceleration and at sensor height 10 % and 30 % (a) Backside dynamic acceleration (b) Frontside dynamic acceleration (c) Backside dynamic pressure (d) Frontside dynamic pressure

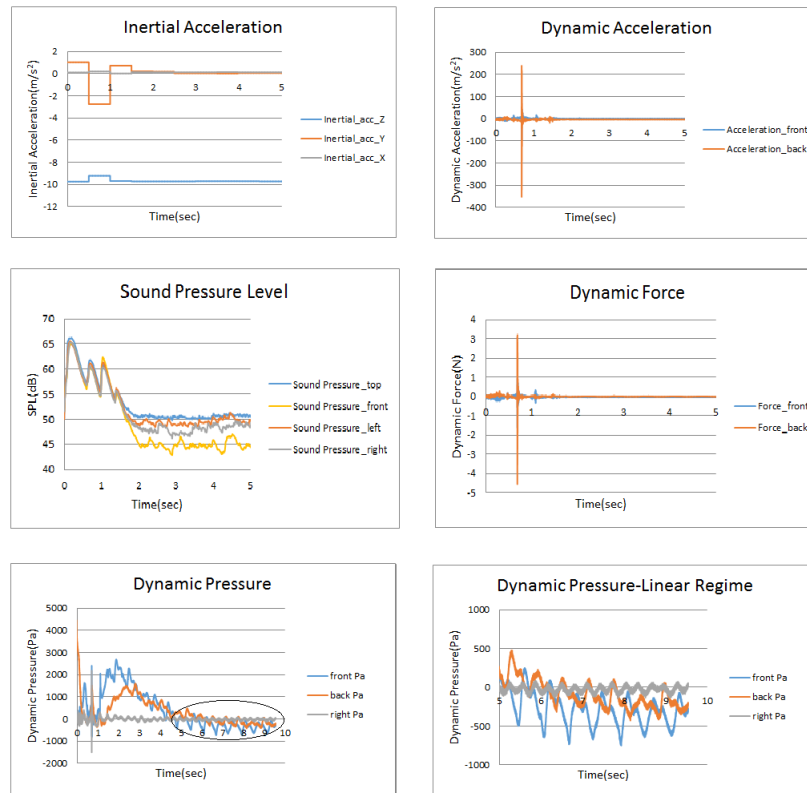6. 40% fill level - deceleration 0.3 g - Sensor height 10% and 30%

Figure 5.16: Experimental results for 40 % fill ,0.3 g deceleration and sensor height 30 % case (a) Inertial acceleration (b) Dynamic acceleration (c) SPL (d) Dynamic Force (e) Dynamic pressure (f) Linear regime in sloshing

Experiment has been performed for 40 % fill level, deceleration 0.3 g and sensor height at 10% and 30% of the tank height. Sensor height is varied to analyse effect of sloshing behavior at different tank height. The required deceleration is obtained based on appropriate dead load selection. Figure. 5.16 shows the recorded test data of tri-axial inertial acceleration data, dynamic force and dynamic acceleration due to wall vibration, radiated sound pressure level, dynamic pressure and sloshing linear regime.

As the vehicle moves in forward direction, fluid rises over front wall. Figure 5.17 (a) shows the condition of fluid at the time of braking that is at 0.499 sec. At this stage, fluid stores its energy in the form of potential energy. SPL data shows peak between starting point of the vehicle and starting point of braking instant corresponds to vehicle motion noise (tyre noise, pulley etc.). As the fluid moves over the front wall, it also hits the back wall as shown in Figure. 5.17 (b). There is strong relation between dynamic force, dynamic acceleration and SPL data, so corresponding noise is referred as hitting noise. Second SPL peak is corresponding to the splashing noise. After impact, due to bubbly flow and nonlinear behavior of fluid as shown in Figure. 5.17
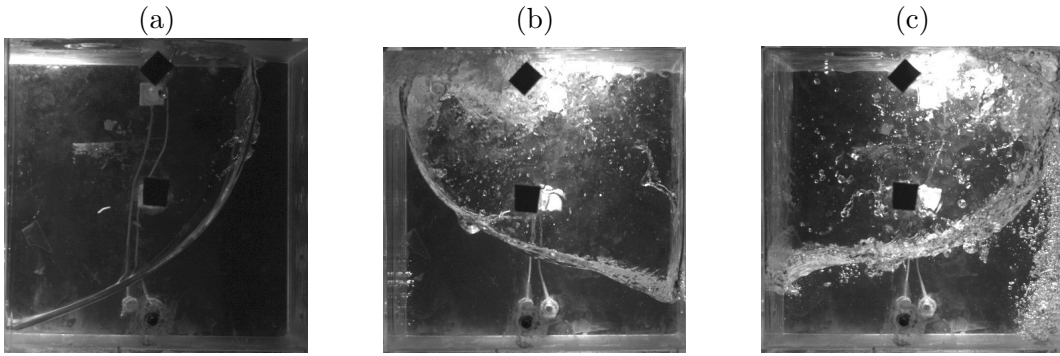
Figure 5.17: 40 % fill, 0.3 g sloshing events(a) event 1 (b) event 2 (c) event 3

(c), no dynamic action is observed in dynamic force and dynamic acceleration but these events captured in dynamic pressure sensor. As the deceleration level is large, these case takes more time to reach linear regime. In linear regime, fluid sloshes with its theoretical sloshing natural frequency.

For 40 % fill case, experiment is performed at two different sensor height i.e. 10 % and 30 % as shown in Figure 5.18. By comparing these two cases, it is observed that most of the dynamic events are captured in sensors that are kept at 30% height. But, as the deceleration level is large (0.3 g) compared to above two cases like 0.2 g and 0.25 g , more dynamic action can be observed at same sensor location. Dynamic pressure data shows, good difference in magnitude and phase of dynamic pressure, as it senses fluid motion directly. Dynamic acceleration and dynamic force data senses the wall vibration so, force and acceleration sensor at 10 % height can show dynamic event inphase with sensor at 30 % height. Sound pressure level is independent of sensor height hence it is not considered for sensor mounting height effect.
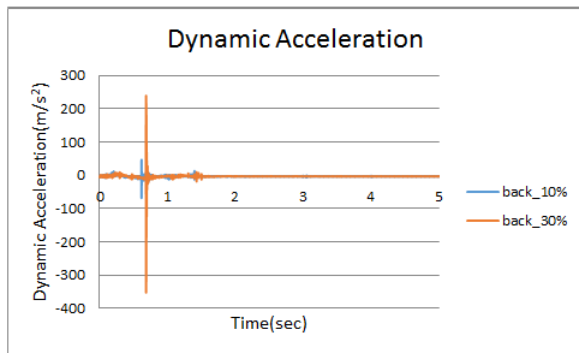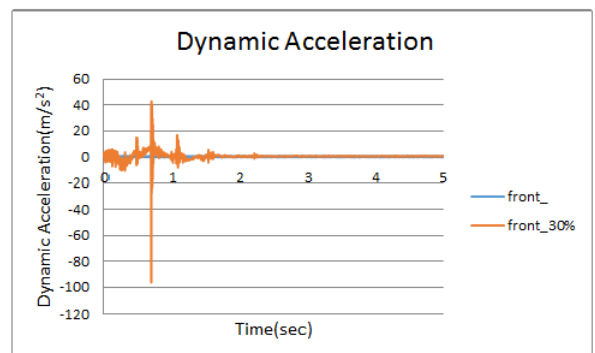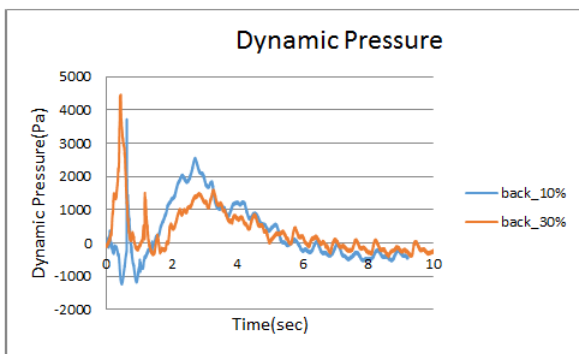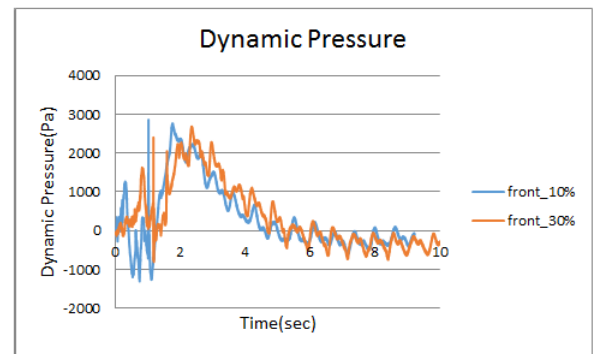
Figure 5.18: Comparison of sloshing behavior for 40% fill level, 0.3 g deceleration and at sensor height 10 % and 30 % (a) Backside dynamic acceleration (b) Frontside dynamic acceleration (c) Backside dynamic pressure (d) Frontside dynamic pressure

7. 60% fill level - deceleration 0.2 g - Sensor height 10% and 50%

Figure 5.19: Experimental results for 60 % fill and 0.2 g deceleration and sensor height 50 % case (a) Inertial acceleration (b) Dynamic acceleration (c) SPL (d) Dynamic Force (e) Dynamic pressure (f) Linear regime in sloshing

Experiment has been performed for 60 % fill level, deceleration 0.2 g and sensor height at 10% and 50% of the tank height. Sensor height is varied to analyse effect of sloshing behavior at different tank height.The required deceleration is obtained based on appropriate dead load selection. Figure 5.19 shows the recorded test data of tri-axial inertial acceleration data, dynamic force, dynamic acceleration due to wall vibration, radiated sound pressure level, dynamic pressure due to fluid impact, and sloshing linear regime.

As the vehicle moves in forward direction fluid rises over front wall. Figure 5.20 (a) shows the condition of fluid at the time of braking i.e. at 0.499 sec. At this stage, fluid stores its energy in the form of potential energy. SPL data shows peak between starting point (0 sec) of the vehicle and starting point of braking instant (0.499 sec) that corresponding to vehicle motion noise (tyre noise, pulley etc.).

After braking, the fluid that has climbed over the front wall hits the top corner of back wall. This makes a tremendous impact as sensed by all the dynamic acceleration, dynamic force, dynamic pressure and sound pressure level data. As the fluid hits the
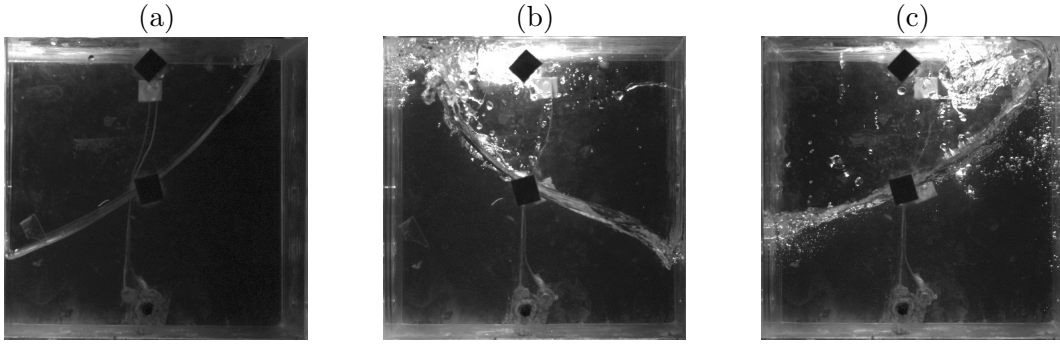
Figure 5.20: 60 % fill, 0.2 g sloshing events(a) event 1 (b) event 2 (c) event 3

top corner of back wall as shown in Figure. 5.20 (b) dynamic sensors on back wall like dynamic force, dynamic acceleration and dynamic pressure shows maximum peak value than front. After completion of back hitting, fluids moves towards front wall as shown in Figure 5.20 (c) in smaller magnitude. As fluid hits the top wall, vibrations are transfered to the front sides. Dynamic force and dynamic acceleration sensor on front wall senses this event in smaller magnitude but in same phase. By using high speed camera images fluid hitting on top wall observed and corresponding noise is observed in SPL data.

Sloshing fluid mass includes rigid mass and modal mass, rigid mass doesn't take part in fluid sloshing. As the fill level increases rigid mass goes on increasing. For higher fill level due to large inertia, fluid approach linear regime from impacting regime in lesser duration of time. Here, fluid reaches to linear regime in less time compared to 20 % and 40 % fill cases. In linear regime, fluid sloshes with same amplitude and front and back peaks are completely out of phase. The sloshing frequency in this case is validated with theoretical sloshing natural frequency.

Experiment is performed at two different sensor height i.e. 10 % and 50 % as shown in Figure. 5.21. By comparing these two cases, it is observed that most of the dynamic events are captured in sensors that are kept at 50% height. There is significant difference in magnitude of dynamic pressure on back and front wall, in these two cases. Dynamic pressure sensor at 50 % shows peak with more magnitude and with slight phase difference compared to 10% sensor. Dynamic acceleration at 50 % shows peak almost inphase with dynamic acceleration at 10 % . As impact is not significant so both sensors are showing nearly same magnitude as a representaion of wall displacement. Dynamic sound pressure level is independent of sensor height hence it is not considered in sensor mounting effect.

Figure 5.21: Comparison of sloshing behavior for 60% fill level, 0.2 g deceleration and at sensor height 10 % and 30 % (a) Backside dynamic acceleration (b) Frontside dynamic acceleration (c) Backside dynamic pressure (d) Frontside dynamic pressure

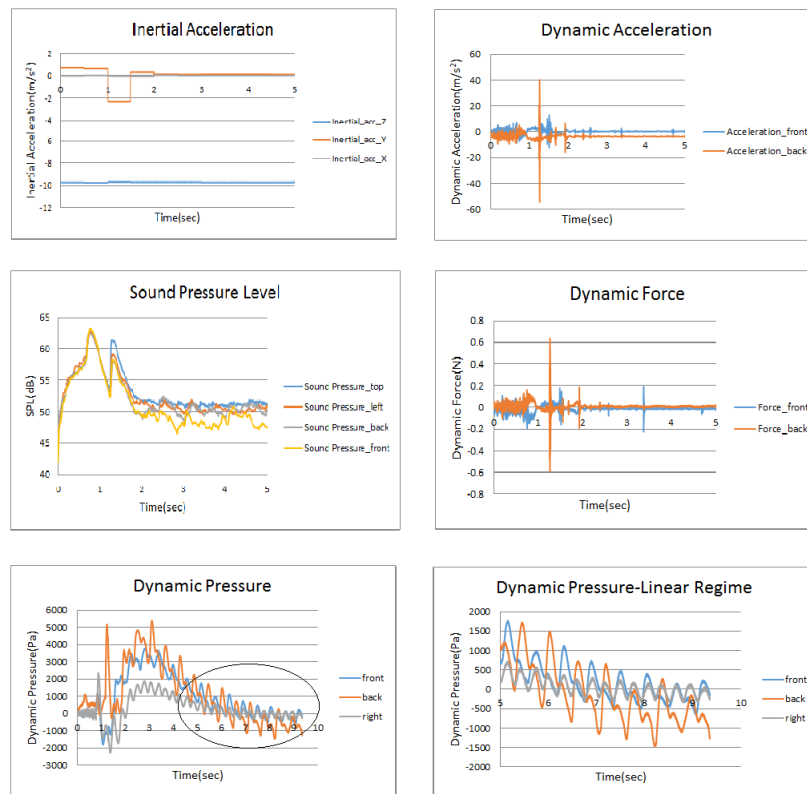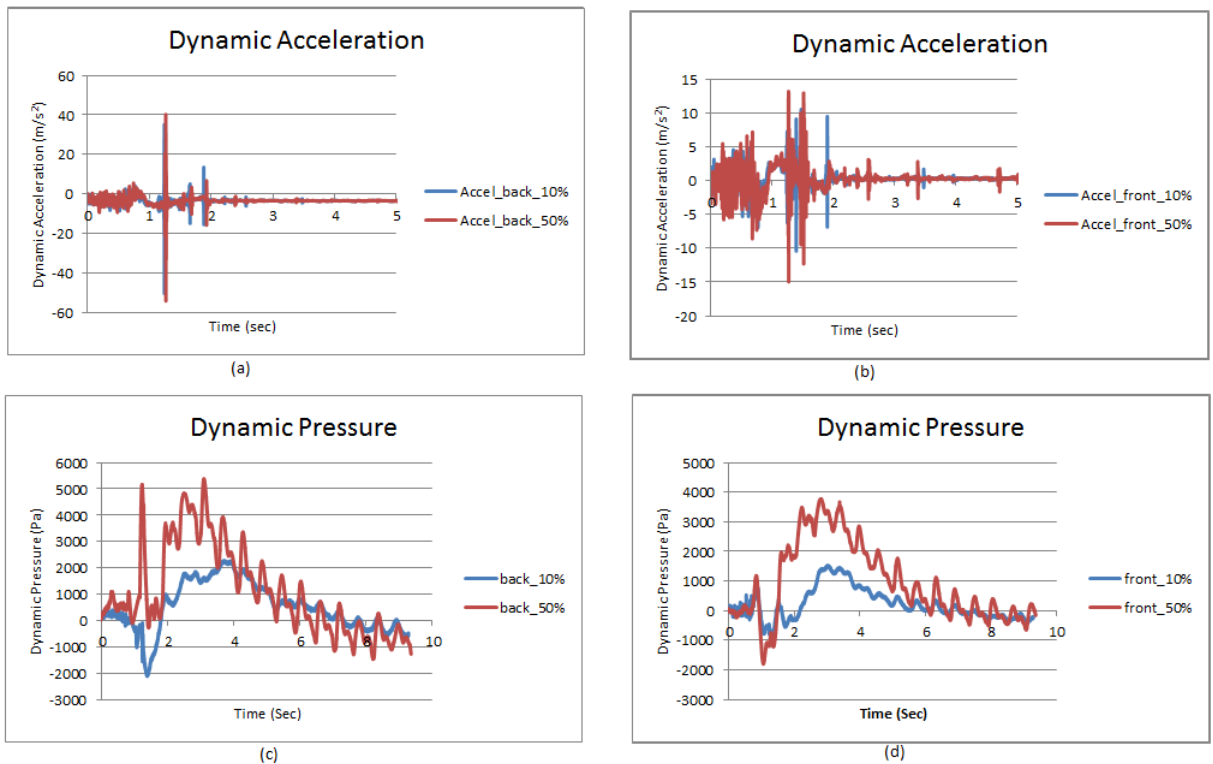8. 60% fill level - deceleration 0.25 g - Sensor height 10% and 50%

Figure 5.22: Experimental results for 60 % fill and 0.25 g deceleration and sensor height 50 % case (a) Inertial acceleration (b) Dynamic acceleration (c) SPL (d) Dynamic Force (e) Dynamic pressure (f) Linear regime in sloshing

Experiment has been performed for 60 % fill level, deceleration 0.25 g and sensor height at 10% and 50% of the tank height. Sensor height is varied to analyse effect of sloshing behavior at different tank height. The required deceleration is obtained based on appropriate dead load selection. Figure 5.22 shows, recorded test data of tri-axial inertial acceleration data, dynamic force and dynamic acceleration due to wall vibration, radiated sound pressure level, dynamic pressure due to fluid impact, and sloshing linear regime.

As the vehicle moves in forward direction fluid moves over front wall. Figure 5.23 (a) shows the condition of fluid at the time of braking means at 0.499 sec. At this stage fluid stores its energy in the form of potential energy. SPL data shows a peak between starting point (0 sec) of the vehicle and starting point of braking instant (0.499 sec) that corresponds to vehicle motion noise (tyre noise, pulley etc.).

After braking , the fluid that has climbed over the front wall then hit to the top corner of back wall as shown Figure 5.23 (b) by making a tremendous impact as sensed by all the dynamic acceleration, dynamic force, dynamic pressure and sound pressure level
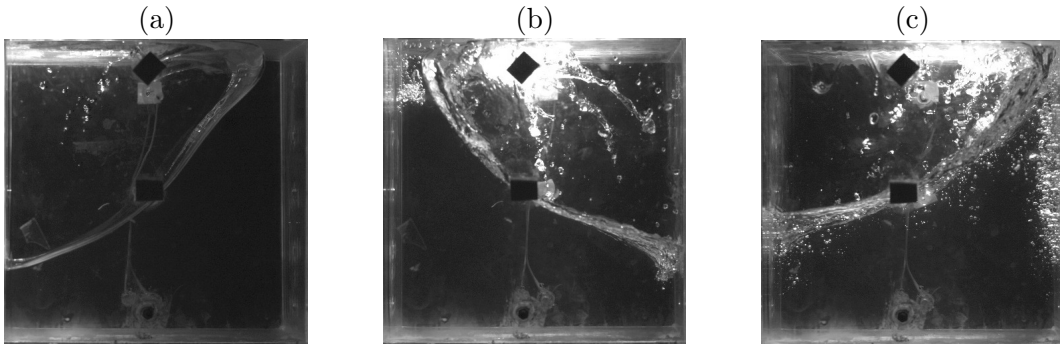
Figure 5.23: 60 % fill, 0.25 g sloshing events (a) event 1 (b) event 2 (c) event 3

data. As the fluid hits the top corner of back wall so dynamic sensors on back wall like dynamic force, dynamic acceleration and dynamic pressure shows, the maximum peak value than front. As it hits the top wall, some vibration are transfered to the front wall. This captured by dynamic force and dynamic acceleration sensor on front wall with lesser magnitude but in phase with back sensors. Figure 5.23 (c) shows, the event of fluid when hits to the top corner of front wall. Second SPL peak is observed at 1.461 sec, and this is due to fluid-fluid interaction. Dynamic pressure sensor captured events but dynamic force and acceleration sensor didn't show any changes. Hence, these are considered not significant structural point of view.

Sloshing fluid mass includes rigid mass and modal mass, rigid mass didn't take part in fluid sloshing. As the fill level increases rigid mass goes on increasing, and also for higher fill level water approaches in linear regime from impacting regime in less duration of time. Here fluid comes to linear regime in less time compared to 20 % and 40 % fill cases. In linear regime, fluid sloshes with same amplitude, front and back peaks are completely out of phase. The sloshing frequency in this case is validated with theoretical sloshing natural frequency.

Experiment is performed at two different sensor height i.e. 10 % and 50 % as shown in Figure. 5.27. By comparing these two cases, it is observed that most of the dynamic events are captured in sensors that are kept at 50% height. There is significant difference in magnitude of dynamic pressure, dynamic acceleration on back and front wall, in these two cases . Dynamic pressure sensor at 50 % shows peak with more magnitude and with slight phase difference compared to 10% sensor. Dynamic Sound pressure level is independent of sensor height hence it is not considered for sensor mounting effects .
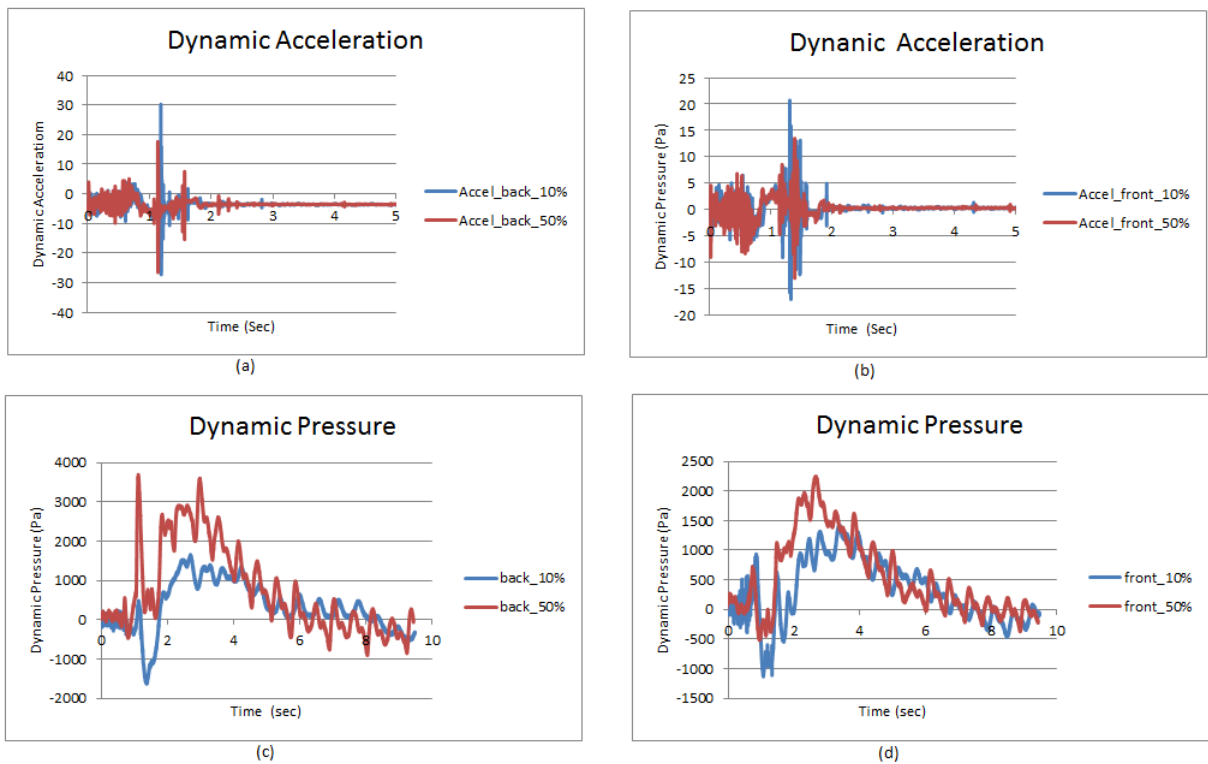
Figure 5.24: Comparison of sloshing behavior for 60% fill level, 0.25 g deceleration and at sensor height 10 % and 50 % (a) Backside dynamic acceleration (b) Frontside dynamic acceleration (c) Backside dynamic pressure (d) Frontside dynamic pressure

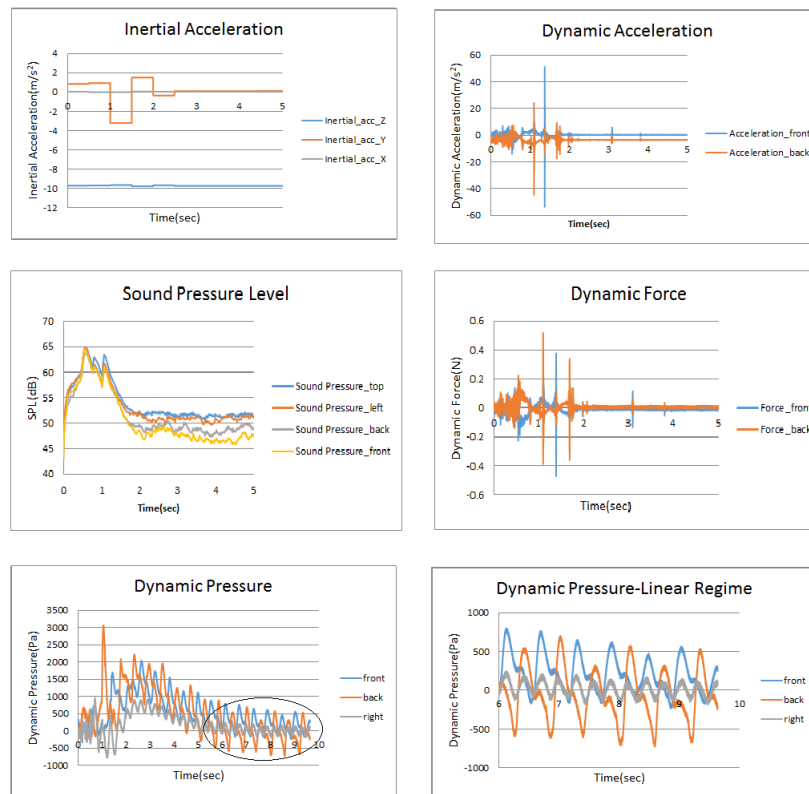9. 60% fill level - deceleration 0.3 g - Sensor height 10% and 50%

Figure 5.25: Experimental results for 60 % fill and 0.3 g deceleration case (a) Inertial acceleration (b) Dynamic acceleration (c) SPL (d) Dynamic Force (e) Dynamic pressure (f) Linear regime in sloshing

Experiment has been performed for 60 % fill level, deceleration 0.3 g and sensor height at 10% and 50% of the tank height. Sensor height is varied to analyse effect of sloshing behavior at different tank height. The required deceleration is obtained based on appropriate dead load selection. Figure 5.25 shows the recorded test data of tri-axial inertial acceleration data, dynamic force, dynamic acceleration due to wall vibration, radiated sound pressure level, dynamic pressure due to fluid impact and sloshing linear regime.

As the vehicle moves in forward direction fluid moves over front wall. At this stage fluid stores its energy in the form of potential energy. SPL data shows peak between starting point (0 sec) of the vehicle and starting point of braking instant (0.499 sec) that corresponding to vehicle motion noise (tyre noise, pulley etc.).

Due to high acceleration and high fill level, fluid rises over the front wall and hits to the top wall at 0.655 sec, as shown in Figure. 5.26(a), while accelerating itself. First sound pressure peak is captured at this event. After braking fluid comes and hits the top corner of the back wall as shown in Figure. 5.26(b), corresponding vibration are

(a)   (b)   (c)
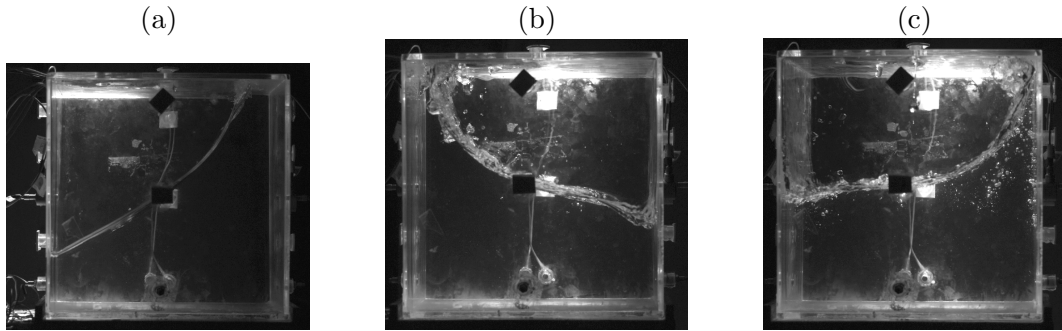
Figure 5.26: 60 % fill, 0.3 g sloshing events(a) event 1 (b) event 2 (c) event 3

captured by dynamic force and dynamic acceleration sensors on back wall and front
wall. Front wall sensors senses vibrations in less maginitude but inphase with back
wall sensors. Second peak in SPL is captured due to this top corner of front wall
hitting as shown in Figure. 5.26 (c). After this instant, no major event is captured in
dynamic force, dynamic acceleration and SPL sensors. Dynamic pressure sensor senses
instantaneous fluid behavior inside the tank. After completion of one cycle, system
reachs to the linear regime and fluid sloshes with theoretical sloshing frequency.
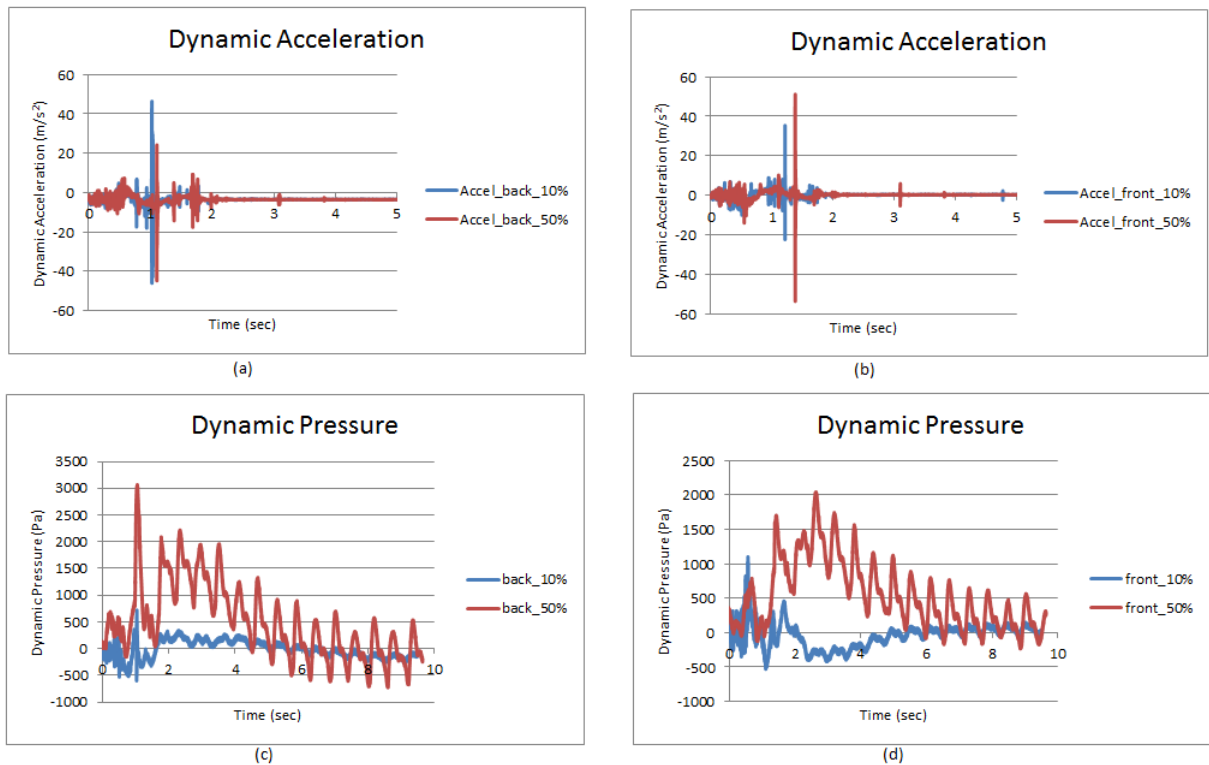
Figure 5.27: Comparison of sloshing behavior for 60% fill level, 0.3 g deceleration and at
sensor height 10 % and 50 % (a) Backside dynamic acceleration (b) Frontside dynamic
acceleration (c) Backside dynamic pressure (d) Frontside dynamic pressure

Experiment is performed at two different sensor height i.e. 10 % and 50 %, as shown in Figure 5.27. By comparing these two cases, it is observed that most of the dynamic events are captured in sensors that are kept at 50% height. There is significant difference in magnitude of dynamic pressure, dynamic force on back and front wall, in these two cases . Dynamic acceleration sensor at 50 % shows peak with more magnitude and with slight phase difference compared to 10% sensor. Dynamic sound pressure level is independent of sensor height hence it is not considered for different sensor mounting effects.

10. 80% fill level - deceleration 0.25 g - Sensor height 10% and 70%
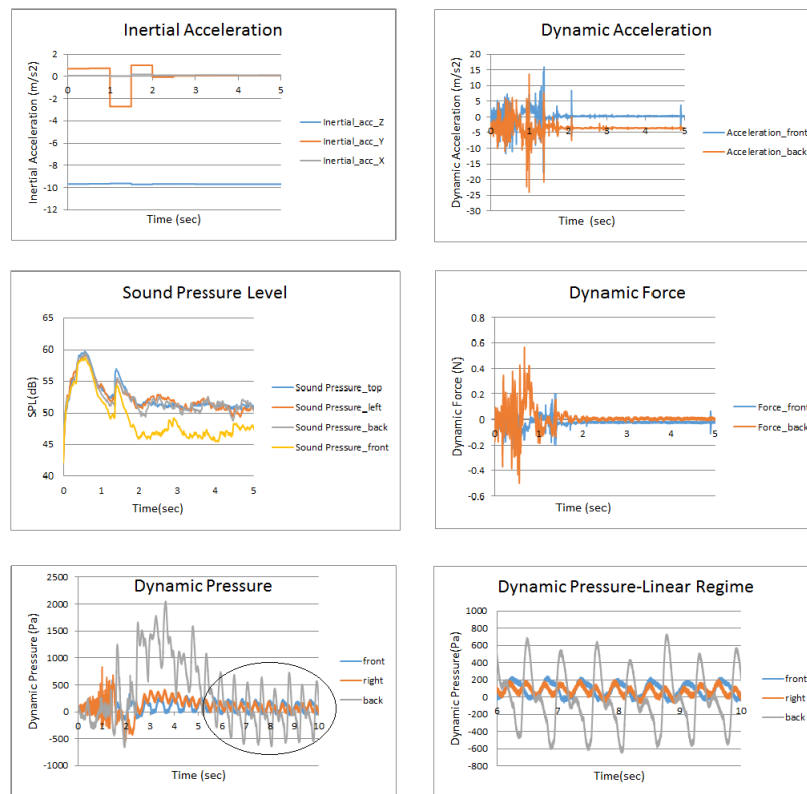
Figure 5.28: Experimental results for 80 % fill , 0.25 g deceleration and sensor height 70 % case (a) Inertial acceleration (b) Dynamic acceleration (c) SPL (d) Dynamic Force (e) Dynamic pressure (f) Linear regime in sloshing

Experiment has been performed for 80 % fill level, deceleration 0.25 g and sensor height 10% and 70% of the tank height. Sensor height is varied to analyse effect of sloshing behavior at different tank height. The required deceleration is obtained based on appropriate dead load selection. Figure 5.28 shows, the recorded test data of tri-axial inertial acceleration data, dynamic force and dynamic acceleration due to wall vibration, dynamic pressure due to fluid impact, and radiated sound pressure level.

The condition of fluid inside the tank at the time of first event at front dynamic pressure sensor when analysed from high speed camera image, as shown in Figure, 5.29 (a) reveales that a major part of fluid has moved towards the front wall . After brake application, the vehicle moved some distance opposite to direction of motion due to elasticity of string used for brake application. This movement of vehicle as described from the inertial acceleration sensor continued for 0.5 sec i.e. from 0.99 sec to 1.49 sec. Background noise (due to vehicle motion, friction) peak is detected in this time duration.
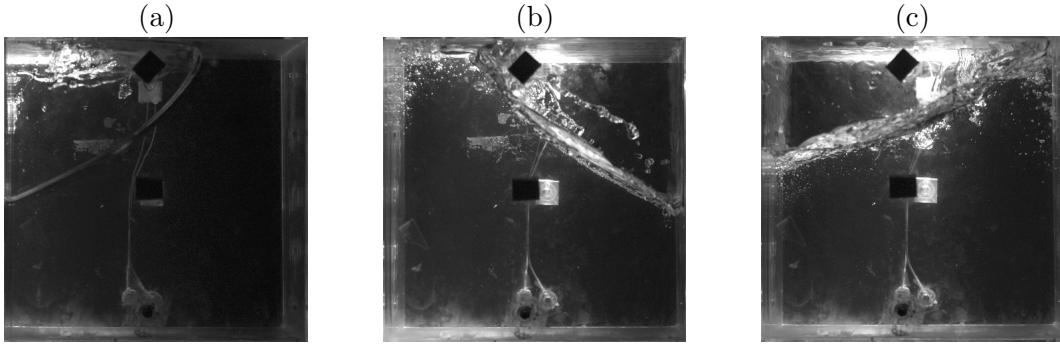
Figure 5.29: 80 % fill, 0.25 g sloshing events(a) event 1 (b) event 2 (c) event 3

As the fill level and deceleration is high therefore non linearity in the fluid behavior is observed. Fluid gets less area to impact on side walls hence clear hitting is not observed. Mostly fluid slides over the wall and in between hits the top wall at the corners. At 0.996 sec, fluid hits top corner of back wall as shown in Figure 5.29 (b) and corresponding dynamic peaks are captured on back wall sensors. But at this instant SPL didn't show the peak because of smooth impact of fluid on back wall. Sloshing behaviors is mixing of spash and hitting. At 1.37 sec, water hits to the top corner of the front wall as shown in Figure 5.29 (c), and corresponding SPL is recorded. Wall displacement due to wave hitting on wall is captured by dynamic force and dynamic acceleration sensors. Dynamic pressure senses the fluid behavior more correctly as it is directly in contact with fluid.

Experiment is performed at two different sensor height i.e. 10 % and 70 %, as shown in Figure 5.30. By comparing these two cases, it is observed that most of the dynamic events are captured in sensors that are kept at 70% height. There is significant difference in magnitude of dynamic back pressure between these two cases. Front dynamic pressure shows peak with phase difference. Dynamic acceleration and dynamic force are almost inphase as they represent wall vibrations. No pure dynamic impact observed for 80 % fill so acceleration and force sensors at different sensors height shows almost same magnitude. Sound pressure level is independent of sensor height hence it is not a considered for sensor mounting effect. Sensor at 10 % height senses events but it is difficult to correlate these events with high speed camera image. As the sensor at 10 % is always dips in fill level, to find the the exact fluid behavior at lower level there is need to use other measures (PIV) to capture these events. Sloshing fluid mass includes rigid mass and modal mass, rigid mass doesn't take part in fluid sloshing. As the fill level increases rigid mass goes on increasing. For higher fill level fluid approach in linear regime from impacting regime by taking less duration of time. Here, fluid reaches to linear regime in less time compared to 20 % , 40 % and 60 % fill cases. In linear regime, fluid sloshes with same amplitude and front and back peaks are completely out of phase. The sloshing frequency in this case is validated with

theoretical sloshing natural frequency.
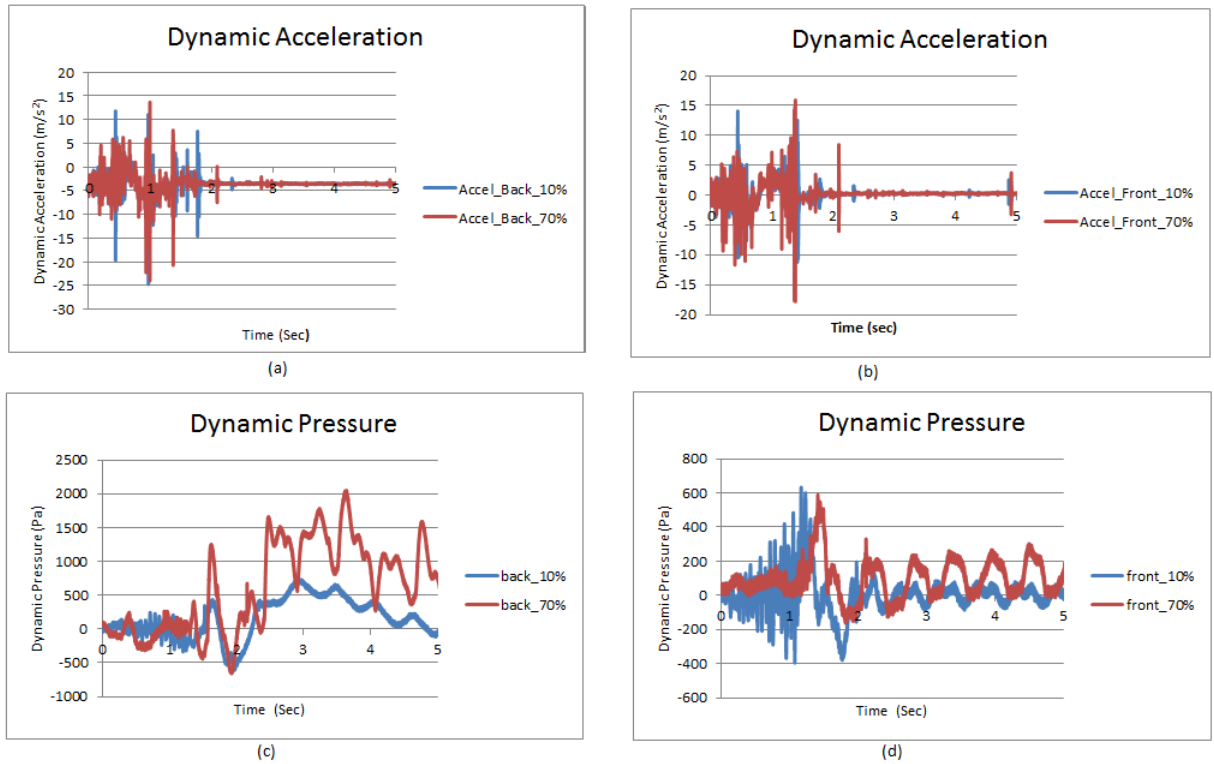

Figure 5.30: Comparison of sloshing behavior for 80% fill level, 0.25 g deceleration and at sensor height 10 % and 70 % (a) Backside dynamic acceleration (b) Frontside dynamic acceleration (c) Backside dynamic pressure (d) Frontside dynamic pressure

5.1.6 Wavelet analysis

Wavelet analysis has attracted attention for its ability to analyze rapidly changing transient signals. Any application using the Fourier transform can be formulated using wavelets to provide more accurately localized temporal and frequency information [19].
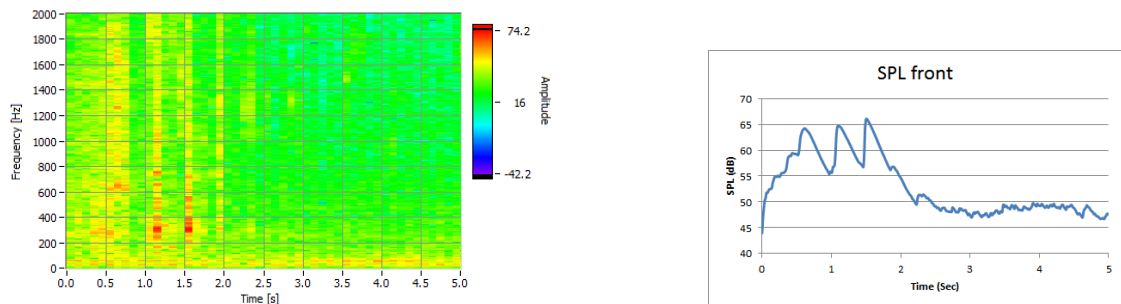
Figure 5.31: Wavelet analysis for 20 % fill cases (a) STFT plot (b) SPL in time domain

Wavelet analysis is suitable to classify different sloshing noise i.e hitting noise, clonk noise and splash noise. From wavelet analysis, it is clear that hitting noise is low frequency

57

noise. For 20% fill and 0.25 g case, first hitting is happened on back wall at 1.2 sec and then on front wall at 1.5 sec. In wavelet analysis also at same time that hitting event is recorded, as shown in Figure 5.31

5.2 Effect of parameters on sloshing

In previous section, explained study of sloshing in rectangular tank is performed for different fill level and different deceleration level. In this section, effect of these parameters on principle component parameters are observed. In principle component peak values of dynamic acceleration, dynamic force and SPL are considered.

5.2.1 Effect of deceleration on sloshing parameters

Figure 5.32: Effect of deceleration level on sloshing parameters (a) Dynamic acceleration (b) Dynamic force (c) SPL

Figure. 5.32 shows the variation of dynamic acceleration and dynamic force on front and back wall and variation of radiated SPL with different deceleration.

Dynamic acceleration and dynamic force represent the wall vibration and both are showing result in phase. Major hitting has been taken place on back wall So, back wall sensors are senses data in higher magnitude than front wall sensors. For 0.2g and 0.25g deceleration

force and acceleration magnitudes are less compared to 0.3g deceleration, there is direct impact on back wall. After hitting the back wall, fluid slides over top wall and hits the front wall. For higher deceleration 0.3 g, after hitting to back wall, fluid distributes and hits on the top corner of front wall and returns to the back wall. As this is a secondary peak so, front side sensors shows values in less magnitude.

Radiated SPL is directly related to the wall displacement. Dynamic back side sensors shows dispacement in higher magnitude. SPL data is in phase with dynamic data on back sensors.
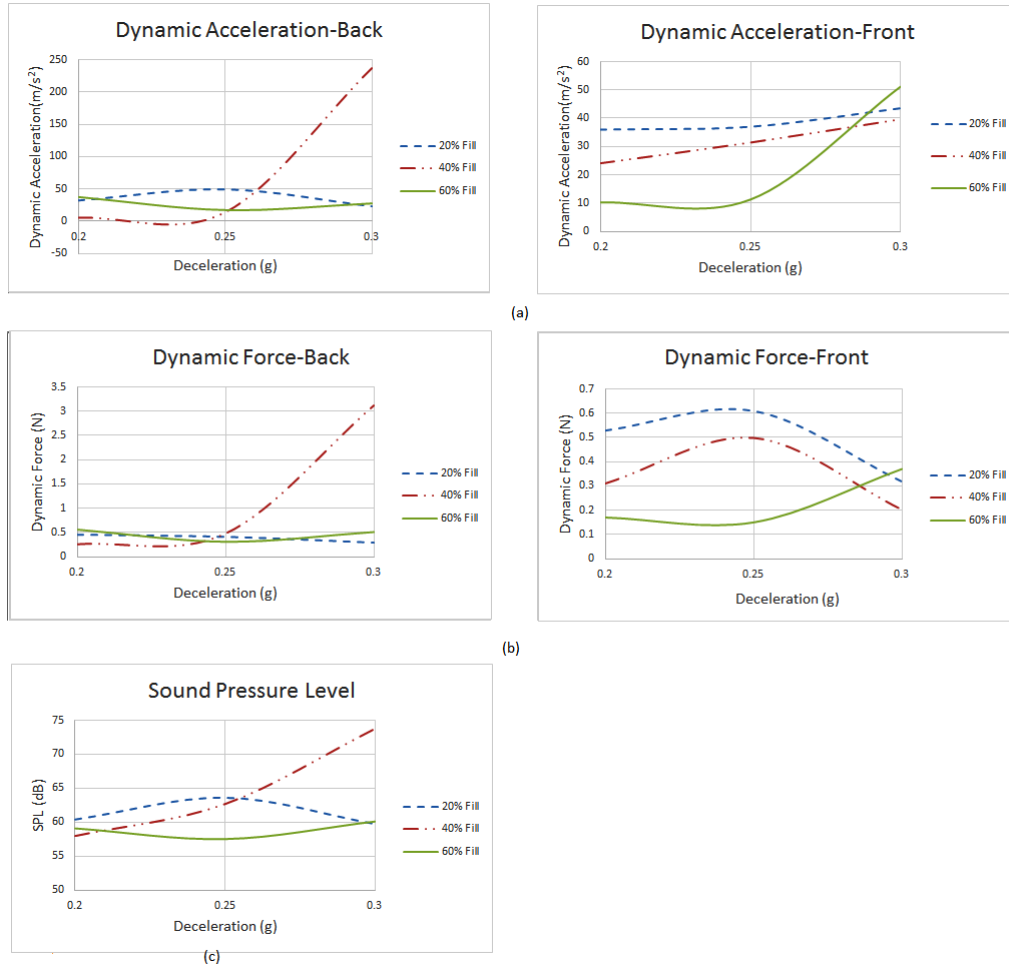
5.2.2 Effect of fill level on sloshing parameters
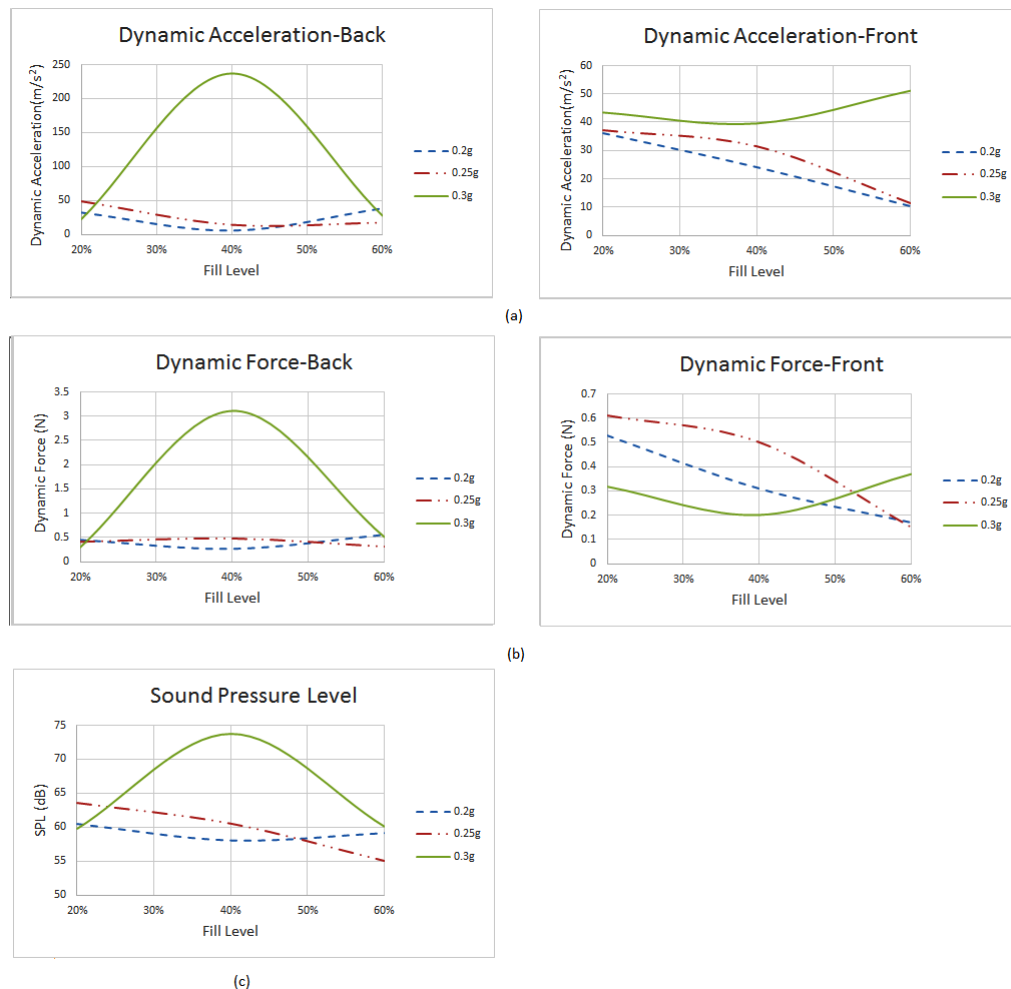

Figure 5.33: Effect of fill level on sloshing parameters (a) Dynamic acceleration (b) Dynamic force (c) SPL

Figure. 5.33 shows, the variation of sloshing parameters with respect to fill level.

Dynamic acceleration amd dynamic force data is in phase because they are corresponding to the wall dispacement. For 40% fill and 0.25g deceleration, major peak is observed because

60

at this instant fluid directly hits on the wall (near sensor location) at higher velocity. For 0.25g and 20 % fill, fluid smoothly moves over back wall and hits to top wall, while for 60 % fill, not directly hitting to back wall is observed. Compared to back wall, front wall sensors shows peak in lower magnitude. Also on front wall, Dynamic acceleration and force at higher deceleration (0.3g) and higher fill (60 % fill) shows higher values compared to other fill level. This is because of of fluid moves on back wall and hits from top wall.

Sound pressure level is proportional to the wall displacement and it is showing radiated noise proportional to the back wall dispacement.

5.2.3   Repeatability and Error Analysis

Figure. 5.34 shows, error analysis of experimental data for different parameters. Repeatability study have been perform by taking three readings of each parameters. Dynamic forces, dynamic acceleration, dynamic pressure and sound pressure level are analysed in experimental analysis. Table 5.2.3 shows standard deviation (σ) and mean values for different parameters and fill level. Experimental error graphs are plotted by taking error values $\pm$ 1 σ.

Table 5.1: Standard deviation of experimental data

|		20 %	40 %	60 %	80 %
Inertial Acceleration (m/s2)	Mean	-2.75	-2.59	-2.7	-2.7
	STDEV	0.03	0.06	0.09	0.1
Front Acceleration (m/s2)	Mean	37.77	31.54	11.89	15.31
	STDEV	4.19	2.9	1.88	4.11
Back Acceleration (m/s2)	Mean	48.02	10.32	17.9	14.94
	STDEV	3.28	4.13	7.05	2.57
Front Force (N)	Mean	0.52	0.49	0.17	0.2
	STDEV	0.08	0.13	0.02	0.03
Back Force (N)	Mean	0.41	0.43	0.31	0.18
	STDEV	0.02	0.05	0.1	0.07
SPL (dB)	Mean	63.17	66.29	56.16	55.18
	STDEV	1.63	2.35	2.34	0.56
Back Pressure (Pa)	Mean	3739.33	1213.22	3778.37	2318
	STDEV	209.92	202.93	588.58	386.66
Front Pressure (Pa)	Mean	3109.93	3007.79	820.67	374
	STDEV	418.85	538.56	203.74	47.13
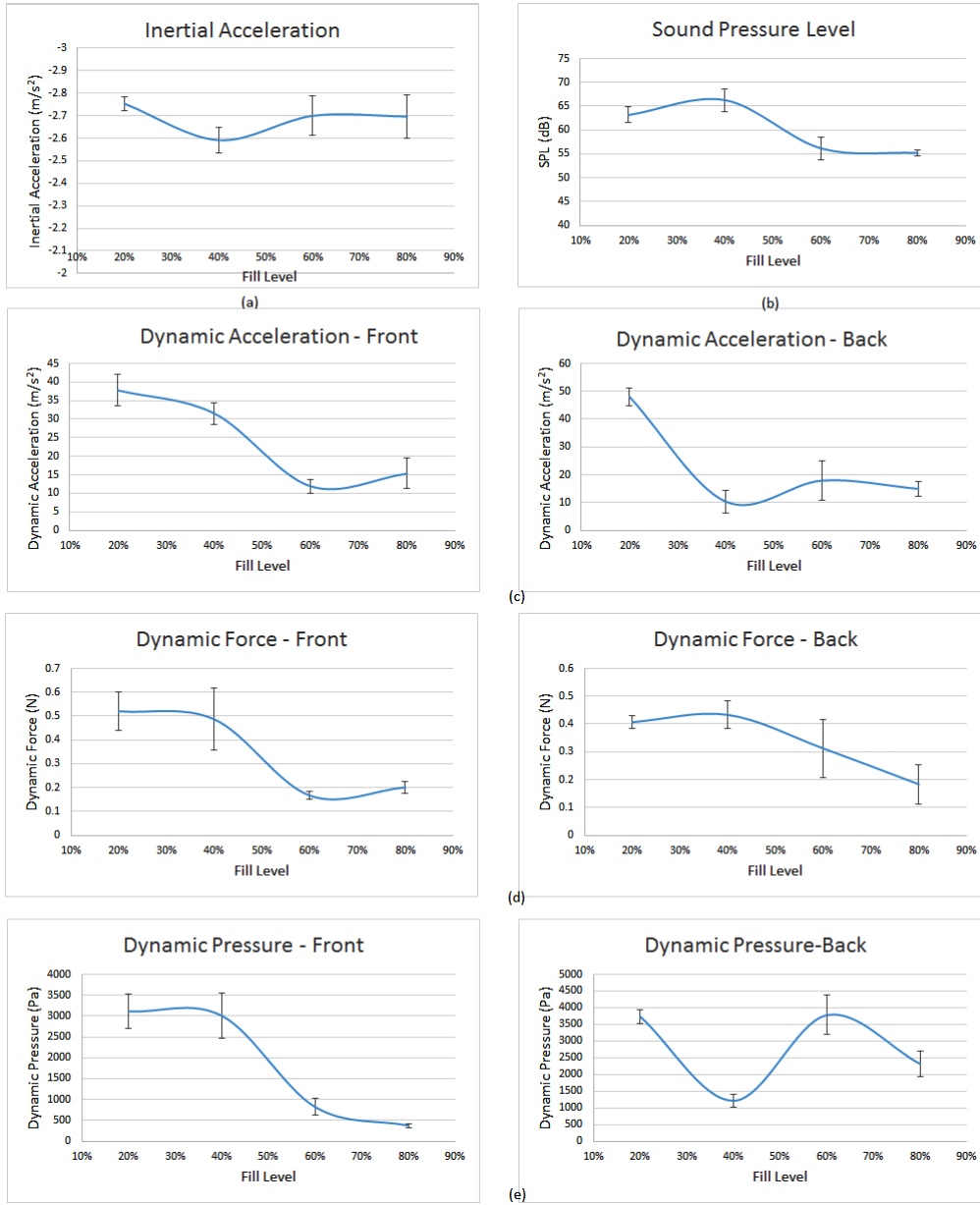
Figure 5.34: Effect of fill level on sloshing parameters (a) Inertial acceleration (b) SPL (c) Dynamic acceleration (d) Dynamic force (e) Dynamic pressure

5.3 Numerical Model Validation approach

Figure.5.35 shows the validation approach of experimental results. Dynamic acceleration data due to wall vibration is validated with structural transient analysis which is done in Ansys. Noise generated due to sloshing captured by microphones is validated with numerical analysis which is done in LMS Virtual.Lab. From experiment, Sloshing natural frequency is measured by observing the peaks in dynamic pressure when it comes in linear regime and is validated with the theoratical sloshing frequency formulae.

The main sloshing event is validated with image correlation analysis.
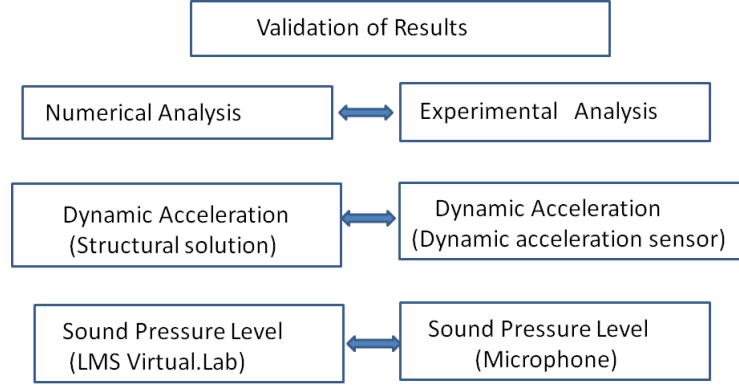
Figure 5.35: Approach for validation of result

1. Sloshing natural frequency

   For linear sloshing, low frequency oscillation maintains periodicty in wave motion. Sloshing natural frequency depends on the dimension of the tank and the fill level.

   Sloshing natural frequency of rectangular tank is given by,

$$f_s = \frac{1}{2\pi}[3.16 * \frac{g}{l}\tanh(3.16 * \frac{h}{l})]^{\frac{1}{2}} \qquad (5.1)$$

   where,

   f_s is sloshing natural frequency,

   l is maximum dimension of the base of the tank,

   h is height of the fluid filled in the tank,

   g is acceleration due to gravity.

Table 5.3 shows the theoratical and experimental sloshing natural frequencies and sloshing period for different fill level.

Table 5.2: Sloshing natural frequency at different filled level

Fill Level	Sloshing natural frequency (Hz)		Sloshing Period (Sec)	
	Theoretical	Experimental	Theoretical	Experimental
20 %	1.35	1.316	0.74	0.76
40 %	1.67	1.613	0.6	0.62
60 %	1.77	1.754	0.56	0.57
80 %	1.80	1.818	0.55	0.55

For linear sloshing case, theoratical sloshing natural frequency close to the experiment. So, current experimental setup is capable to capture sloshing frequency. But at higher fill level and high deceleration level, there is slight deviation between theoratical and experimental sloshing period. Non-linear sloshing has been observed at higher fill levels.

5.4 Numeriacal Results

5.4.1 FSI Transient structural Analysis

FSI transient analysis is done with commertial softwares ANSYS and STAR CCM+. These two codes are coupled by using MpCCI interface. Data exchange takes place at the interface. Structure responds corresponding to the load applied on it. Figure 5.36 shows the variation of the transient displacement (wall) with applied dynamic pressure on it. Figure 5.36 shows transient analysis curve is completely followed the dynamic pressure path.
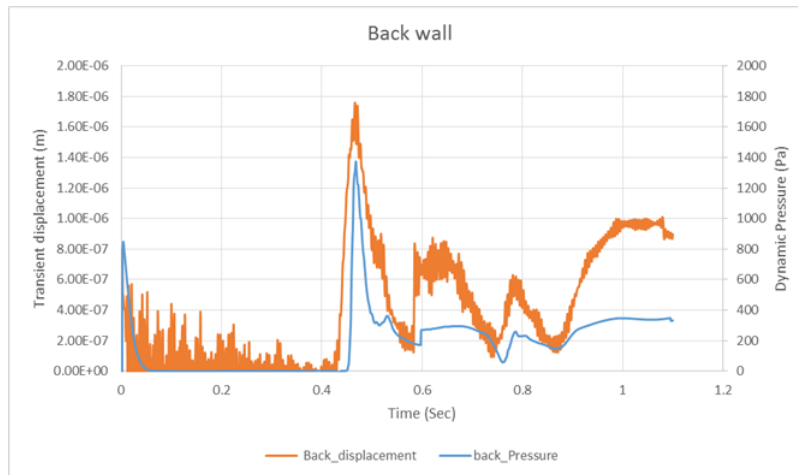

Figure 5.36: Dynamic pressure and transient displacement on back wall for 20% fill and 0.25 g

Transient analysis graph nature is not smooth, this is because of structure can vibrate at different frequency as it has number of natural frequencies. Simulation is run for duration of time as explained

As discussed in section 2.5, FSI simulation can be takes place in two ways, One way

and two way. One way or two way co- simulation approach is selected based on reaction of structure on fluid. If structure is thick, then it is enough to run one way simulation.

In Figure, one way and two way simulation approach are compared based on transient displacement. Difference in peak in two simulation is obseved and it is seen that no significant difference. For this case, it is enough to run only one way simulation.

Hitting noise is observed in lower frequencies i.e. 50 Hz to 500 Hz. In transient analysis, time step is selected based on the interested maximum frequency. For current study, simulation is run for two cases. In first case 1e-3 sec time step is chosen and in second case 0.1 ms time step is chosen. To capture accurate wall velocity and acceleration 1e-4 sec time step is used. Figure 5.37 shows the transient displacement variation at these two cases.
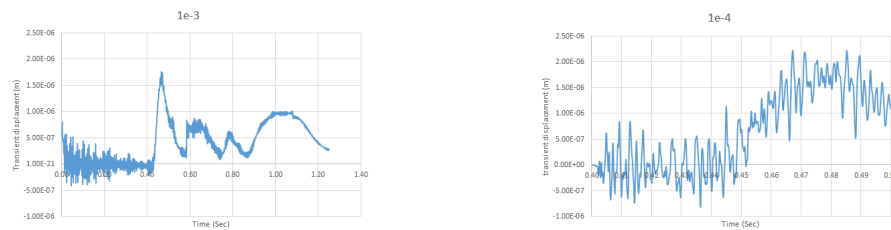

Figure 5.37: Timestep study (a) 1e-3 (b) 1e-4
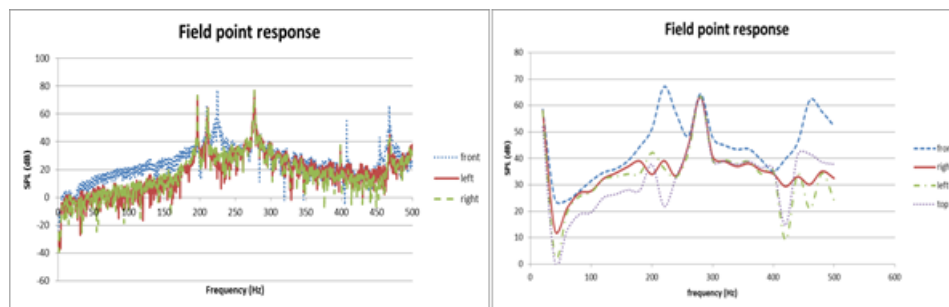
5.4.2 Acoustic harmonic BEM

Figure 5.38: Numerical results (a) 20 % fill (b) 60 % fill

Numerical analysis has been done in accordance to the flowchart discussed in Figure.4.3 using commercial software LMS Virtual. Lab. The calculated total sound pressure level (SPL) results are in good agreement with experimental results. Figure. 5.38 shows the sound pressure spectrum for 20 % and 60 % liquid fill level in the tank at the field points. The chosen field point locations are 130 mm from tank wall. These results generated based on frequency approach. The peak SPL for 20 % fill level in experiments is 77 dB and predicted total SPL is 75 dB and 60 % fill level 77 dB in experiment and 70 dB in simulation. There is a good correlation between experiment and simulation results for 20 % fill but it is not true for 60 % fill level. The main reasons for the discrepancy between experiment and

simulation for 60 % fill level are non-linear sloshing and also the dominance of splash noise. The proposed frequency domain prediction model is good for linear sloshing and also hit noise prediction but not for splash noise. For higher deceleration level (nonlinear), C.G. location of fluid is changes too much and corresponding modes also changes according to that. Means For every instant system changes so the the same mode shapes cant be used throughout simulation so, to predict actual sloshing noise, transient acoustic analysis is to be considered.

5.4.3 Acoustic transient FEM

Acoustic (FEM) transient analysis is done to determined radiated noise in time domain. Acoustic mesh is modelled with 3d solid element. Total number of element Rectangular acoustic mesh is modelled with dimension same as room size. Microphones are located at 1 m distance from the side wall. Transient displacement is mapped on acoustic mesh. For acoustic transient analysis, wall acceleration boundary condition is chosen. Analysis is run to get field point point response of sound. As the sound propagation has directly relation with wall vibration, so radiated noise is in phase with wall acceleration data.
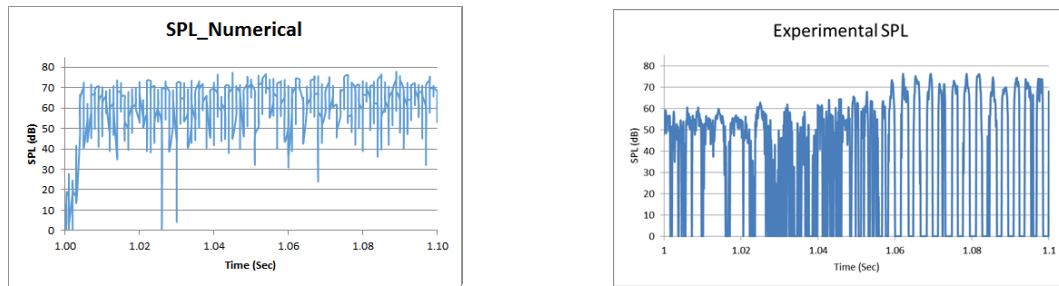
Figure 5.39: SPL in time domain (a) Numerical (b) Experimental

Figure 5.39 shows numerical sound pressure level is validated with experimental sound pressure level. Experimetal sound pressure level shows peak at 1.06 sec with magnitude of 76.39 dB while in simulation 75.3 dB SPL is observed. So, Simulation results are good agreement with experimental results. Methodology can be used for prediction of other acoustic transient analysis problems.

Chapter 6

Summary and Future Scope

6.1   Conclusion

Experimental test setup has been developed to measure liquid sloshing noise under control loading.

An integrated sloshing noise prediction methodology has been developed.

Prediction results from an experiment and simulation have been presented.

Developed experimental setup captured major sloshing events very well and also calculated results are in agreement with experimental results.

Parametric studies have been conducted for fluid fill level and deceleration level. There are three distinct regions have been identified. Major noise generation was happened in the impact region.

6.2   Future Scope

There is scope to improve the theoretical modelling and experimental results for understanding sloshing further.

1. Develop an analytical model to predict the effective sloshing periods for noise generation. Analyze the non-linear sloshing in a rectangular tank.

2. Develop a numerical model for Prediction of splashing noise.

3. Study of sloshing in tanks with different aspect ratios and in the actual automotive fuel tank .

4. The present study can be extended to consider the effect of damping and fill level on structural properties.

References

[1] C. Wachowski, J. Biermann, and R. Schala. Approaches to analyse and predict slosh noise of vehicle fuel tanks. In 24th International Conference of Noise and Vibration Engineering (ISMA2010), Belgium. 2010 .

[2] M. Kamei, J. Hanai, W. Fukasawa, and T. Makino. Establishment of a method for predicting and confirming fuel tank sloshing noise. Technical Report, SAE Technical Paper 2007.

[3] K. Kamiya, Y. Yamaguchi, and E. De Vries. Simulation Studies of Sloshing in a Fuel Tank. *Studies* 2011, (2002) 05–05.

[4] P. De Man and J.-J. Van Schaftingen. Prediction of Vehicle Fuel Tank Slosh Noise from Component-Level Test Data. Technical Report, SAE Technical Paper 2012.

[5] S. aus der Wiesche. Noise due to sloshing within automotive fuel tanks. *Forschung im Ingenieurwesen* 70, (2005) 13–24.

[6] J.-S. Park, S.-C. Choi, and S.-G. Hong. The prediction of fuel sloshing noise based on fluid-structure interaction analysis. *SAE International Journal of Passenger Cars-Mechanical Systems* 4, (2011) 1304–1310.

[7] V. V. S. Vytla and Y. Ando. Fluid Structure Interaction Simulation of Fuel Tank Sloshing. Technical Report, SAE Technical Paper 2013.

[8] L. Khezzar, A. Seibi, and A. Goharzadeh. Water Sloshing in Rectangular Tanks–An Experimental Investigation & Numerical Simulation. *Int. J. of Ingineering (IJE)* 3, (2009) 174–184.

[9] M. Hattori, A. Arami, and T. Yui. Wave impact pressure on vertical walls under breaking waves of various types. *Coastal Engineering* 22, (1994) 79–114.

[10] K. Thiagarajan, D. Rakshit, and N. Repalle. The air–water sloshing problem: Fundamental analysis and parametric studies on excitation and fill levels. *Ocean Engineering* 38, (2011) 498–508.

[11] L. Hou, F. Li, and C. Wu. A numerical study of liquid sloshing in a two-dimensional tank under external excitations. *Journal of Marine Science and Application* 11, (2012) 305–310.

[12] M. Peric and T. Zorn. Simulation of sloshing loads on moving tanks. In ASME 2005 24th International Conference on Offshore Mechanics and Arctic Engineering. American Society of Mechanical Engineers, 2005 1017–1026.

[13] O. Jaiswal, S. Kulkarni, and P. Pathak. A study on sloshing frequencies of fluid-tank system. In Proceedings of the 14th World Conference on Earthquake Engineering. 2008 12–17.

[14] G. J. DeSalvo and J. A. Swanson. ANSYS user's manual. *Swanson Analysis Systems* .

[15] S. U. Manual. LMS International. *Leuven, Belgium* .

[16] D. A. Bies and C. H. Hansen. Engineering noise control: theory and practice. CRC Press, 2009.

[17] S. Fraunhofer. MpCCI: Multidisciplinary Simulations through Code Coupling, Version 3.0. *MpCCI Manuals* .

[18] F.-K. Benra, H. J. Dohmen, J. Pei, S. Schuster, and B. Wan. A Comparison of One-Way and Two-Way Coupling Methods for Numerical Analysis of Fluid-Structure Interactions. *Journal of applied mathematics* 2011.

[19] D. T. Lee and A. Yamamoto. Wavelet analysis: theory and applications. *Hewlett Packard journal* 45, (1994) 44–44.